Research Paper



GEOSPHERE

GEOSPHERE; v. 11, no. 4

doi:10.1130/GES01152.1

6 figures; 6 tables; 1 supplemental file

CORRESPONDENCE: cborrelli@ur.rochester.edu

CITATION: Borrelli, C., and Katz, M.E., 2015, Dynamic deep-water circulation in the northwestern Pacific during the Eocene: Evidence from Ocean Drilling Program Site 884 benthic foraminiferal stable isotopes ($\delta^{18}O$ and $\delta^{13}C$): Geosphere, v. 11, no. 4, p. 1204–1225, doi:10.1130/GES01152.1.

Received 12 November 2014
Revision received 10 April 2015
Accepted 21 May 2015
Published online 10 June 2015



# Dynamic deep-water circulation in the northwestern Pacific during the Eocene: Evidence from Ocean Drilling Program Site 884 benthic foraminiferal stable isotopes ($\delta^{18}O$ and $\delta^{13}C$)

**C. Borrelli* and M.E. Katz**

Department of Earth and Environmental Sciences, Rensselaer Polytechnic Institute, Jonsson-Rowland Science Center, 1W19, 110 8th Street, Troy, New York 12180, USA

## ABSTRACT

**New benthic foraminiferal $\delta^{18}O$ and $\delta^{13}C$ data from Ocean Drilling Program (ODP) Site 884 (northwestern Pacific) add significant structure to a previous lower resolution record; our higher resolution detail and comparisons with published isotopic records provide new insights into paleoceanographic changes in the northwestern Pacific from the middle Eocene to the early Oligocene.**

**From the early-middle until the mid-middle Eocene (ca. 49–43 Ma), a comparison of the Site 884 $\delta^{18}O$ values with published ODP $\delta^{18}O$ records from the Pacific (Site 1218), Atlantic (Site 1260), and Southern Ocean (Site 689) reveals that these basins were bathed by a common water mass, probably originating from the Southern Ocean, or by different water masses having a similar $\delta^{18}O$ signature. From the mid-middle until the early-late Eocene (ca. 42–37 Ma), the Site 884 record reveals increasing complexity in deep-water circulation. The relatively low Site 884 $\delta^{18}O$ values suggest that the northwestern Pacific was bathed by a water mass that was warmer than at the other Pacific, Atlantic, and Southern Ocean sites used in this study. Based on the relatively low $\delta^{13}C$ values at Site 884, there are two possible scenarios for the origin of this northwestern Pacific water mass: (1) nutrient-rich surface waters downwelling at the higher latitudes of the North Pacific (Bering Sea); or (2) warm saline deep waters originating at low latitudes (possibly from the Tethys). In the late Eocene (ca. 36.5 Ma), the Site 884 $\delta^{18}O$ and $\delta^{13}C$ values increased, becoming more similar to Sites 1218 (Pacific), 1053 (Atlantic), and 689 (Southern Ocean), indicating an additional change in deep-water circulation, with a deep-water mass originating from the Southern Ocean bathing the northwestern Pacific.**

## INTRODUCTION

The initiation of one of the most important climatic and oceanographic transitions of the past 50 m.y. occurred from the late-middle Eocene to the early Oligocene (ca. 40–33 Ma), when (1) the small to nonexistent ice sheets of the early Paleogene greenhouse shifted to the continent-scale Antarctic ice sheets in the early Oligocene (e.g., Miller and Fairbanks, 1985; Barron et al., 1991; Ehrmann and Mackensen, 1992; Zachos et al., 1992, 2001; Browning et al., 1996; Kominz and Pekar, 2001; Lear et al., 2004, 2008; Coxall et al., 2005; Miller et al., 2005, 2008a; Katz et al., 2008; Cramer et al., 2009, 2011; Dawber and Tripati, 2011); and (2) the warm temperatures of the early Paleogene gave way to the cooler temperatures of the late Eocene–early Oligocene, as recorded in several proxies, for example planktonic and benthic foraminiferal $\delta^{18}O$ (e.g., Zachos et al., 1994; Diester-Haass and Zahn, 1996; Miller et al., 2008b; Cramer et al., 2009); planktonic and benthic foraminiferal Mg/Ca (e.g., Lear et al., 2008; Pusz et al., 2011); floral and faunal turnover (e.g., Miller et al., 1992; Thomas, 2007; Wade and Pearson, 2008; Aubry and Bord, 2009); and the organic paleothermometer $TEX_{86}$ (e.g., Liu et al., 2009; Wade et al., 2012).

What triggered the initiation of this climate change is still a matter of debate. Two main events, not mutually exclusive (e.g., Scher and Martin, 2006; Katz et al., 2008), have been proposed to explain this critical climate shift during the Cenozoic: (1) decline in atmospheric greenhouse gases concentration, in particular $CO_2$ (e.g., DeConto and Pollard, 2003; Pearson et al., 2009; Pagani et al., 2011); and (2) opening of key oceanic gateways, which affected global ocean circulation (Scher and Martin, 2006; Livermore et al., 2007; Exon et al., 2004; Stickley et al., 2004; Cramer et al., 2009; Katz et al., 2011; Borrelli et al., 2014).

In the first case, declining atmospheric $CO_2$ was invoked as the primary mechanism that triggered cooling and development of continental-scale Antarctic ice sheets (e.g., DeConto and Pollard, 2003; Tripati et al., 2005; Pearson et al., 2009; Pagani et al., 2011). As summarized by DeConto and Pollard (2003), a decrease in $pCO_2$ led to cooling, which progressively favored snow accumulation over Antarctica at higher elevations, in particular during orbital periods conducive to snow accumulation and ice-sheet growth. Planktonic foraminiferal boron isotope and alkenone-based $pCO_2$ reconstructions (Pearson et al., 2009; Pagani et al., 2011) indicate a decline in $pCO_2$ in the late-late Eocene to early Oligocene (ca. 34–33.6 Ma). Even if the absolute concentration of $CO_2$ in the atmosphere is difficult to estimate, both Pearson et al. (2009) and Pagani et al. (2011) concluded that the relatively small decrease in atmospheric $CO_2$

*Present address: Department of Earth and Environmental Sciences, University of Rochester, 227 Hutchison Hall, P.O. Box 270221, Rochester, New York 14627, USA.

concentration at the Eocene-Oligocene boundary was a critical condition for the global cooling and the development of ice sheets on Antarctica, supporting the conclusions of modeling simulations (DeConto and Pollard, 2003; DeConto et al., 2008).

In the second case, Antarctic glaciation could have been triggered by the opening of two critical ocean gateways: the Drake Passage (ca. 41 Ma; Scher and Martin, 2006; Livermore et al., 2007), which isolated Antarctica from South America, and the Tasman Rise, which isolated Antarctica from Australia (starting before 35.5 Ma; Exon et al., 2004; Stickley et al., 2004; possibly as early as 49–50 Ma; Bijl et al., 2013). The opening of these two gateways allowed the development of the Antarctic Circumpolar Current (ACC). Today, the ACC (1) creates a barrier to southward flow of subtropical surface water of the subtropical gyre (e.g., Toggweiler and Bjornsson, 2000; Sijp and England, 2004, 2005); (2) leads to thermal isolation of Antarctica and to a net heat transfer from the Southern to the Northern Hemisphere (e.g., Nong et al., 2000; Toggweiler and Bjornsson, 2000, Sijp and England, 2004); and (3) is a component of the Atlantic meridional overturning circulation (e.g., Cox, 1989; Toggweiler and Samuels, 1995; Toggweiler and Bjornsson, 2000; Sijp and England, 2005), even if its role in driving the northern cell of the meridional overturning circulation is not yet resolved (Kuhlbrodt et al., 2007). Several studies suggest a correlation between the opening of the Drake Passage and/or Tasman Rise, and consequent development of a current around the Antarctic continent, and changes in global climate and ocean productivity, temperature, and circulation (e.g., Diester-Haass and Zahn, 1996; Scher and Martin, 2006, 2008; Cramer et al., 2009; Miller et al., 2009; Katz et al., 2011; Borrelli et al., 2014).

Today, the Pacific Ocean is Earth's largest basin and it has been a key component of climate evolution since the early Cenozoic (65–0 Ma; see Lyle et al., 2008, for a review). Considering that the early Cenozoic Pacific Ocean was even larger than today (as reviewed in Lyle et al., 2008), understanding Pacific Ocean circulation from the middle Eocene to the early Oligocene (ca. 49–33 Ma) is a fundamental step toward better constraining the impact of this basin on the evolution of Earth's climate during the middle Cenozoic (Lyle et al., 2008).

The investigation of benthic foraminiferal (bf) stable oxygen and carbon isotopes ($\delta^{18}O_{bf}$ and $\delta^{13}C_{bf}$) is one of the tools used to reconstruct past changes in ocean circulation (e.g., Curry and Lohmann, 1982; Oppo and Fairbanks, 1987; Miller, 1992; Wright et al., 1992; Zachos et al., 2001; Cramer et al., 2009). This is possible because changes in $\delta^{18}O_{bf}$ values reflect temperature and oxygen isotopic composition of the seawater ($\delta_w$) in which foraminifera calcify, whereas changes in $\delta^{13}C_{bf}$ are influenced primarily by carbon exchange among different reservoirs (e.g., atmosphere, biosphere, ocean, sediments) and mixing among different water masses. As reviewed by Cramer et al. (2009), each water mass started to be characterized by a narrow range of $\delta^{13}C_{bf}$ values beginning in the middle Miocene. Therefore, $\delta^{13}C_{bf}$ values can be used as tracers of different water masses in Neogene paleoceanographic reconstructions (e.g., Curry and Lohmann, 1982; Oppo and Fairbanks, 1987; Woodruff and Savin, 1989; Billups et al., 2002; Hodell and Venz-Curtis, 2006; Poore et al., 2006). AABW is characterized by relatively low $\delta^{13}C$ because of its nutrient-rich Circumpolar Deep Water component; North Atlantic Deep Water (NADW) is characterized by relatively high $\delta^{13}C$ because of the downwelling of nutrient-poor surface waters at the higher latitudes of the North Atlantic; and Pacific water is characterized by the lowest $\delta^{13}C$ because of the accumulation of nutrients sinking from the surface over a long flow path (Kroopnick, 1985).

Using modern Neogene $\delta^{13}C_{bf}$ patterns as an analog for Eocene paleoceanographic reconstructions requires several assumptions (e.g., water mass characteristic and circulation path similar to today; Borrelli et al., 2014). For the middle Eocene–early Oligocene, Cramer et al. (2009) showed that $\delta^{18}O_{bf}$ values were different in different ocean basins, whereas $\delta^{13}C_{bf}$ values were fairly uniform; however, Borrelli et al. (2014) demonstrated that an initial differentiation in $\delta^{13}C_{bf}$ values between Southern Ocean (Ocean Drilling Program, ODP Site 689) and northwestern Atlantic (ODP Site 1053) started to develop in the late-middle Eocene (ca. 38 Ma). These studies demonstrated that $\delta^{13}C_{bf}$ values can be used to refine the $\delta^{18}O_{bf}$ interpretation of ocean circulation in the middle Eocene–early Oligocene in those cases in which a $\delta^{13}C_{bf}$ gradient is present among different water masses. (For details about the applicability of modern $\delta^{13}C_{bf}$ patterns to identify middle Eocene–early Oligocene deep-water masses, see the Discussion section, Overview on the Use of $\delta^{18}O_{bf}$ and $\delta^{13}C_{bf}$ .)

In order to better (1) constrain the ocean circulation in the northwestern Pacific from the middle Eocene to the early Oligocene and (2) place the ocean circulation in the northwestern Pacific in the context of a global ocean circulation path, we selected several sites from different oceans (northwestern and equatorial Pacific, Atlantic, and Southern Oceans) with benthic foraminiferal $\delta^{18}O_{bf}$ and $\delta^{13}C_{bf}$ records coeval with this study (ca. 49–33 Ma). The benthic foraminiferal stable isotopic records from ODP Site 884 were investigated and compared with other published records from the northwestern and equatorial Pacific (ODP Site 883, Pak and Miller, 1995; Site 865, Bralower et al., 1995; Site 1218, Lear et al., 2004; Coxall et al., 2005; Coxall and Wilson, 2011; Site 1209, Dutton et al., 2005; Dawber and Tripati, 2011), the northwestern and western Atlantic (ODP Site 1053, Katz et al., 2011; Borrelli et al., 2014; Site 1260, Sexton et al., 2006), and the Southern Ocean (ODP Site 689, Diester-Haass and Zahn, 1996; Bohaty and Zachos, 2003; Bohaty et al., 2012) (Fig. 1; Table 1).

## MATERIAL AND METHODS

We analyzed benthic foraminifera from middle Eocene to lower Oligocene sections (cores 84–74) from ODP Site 884 Hole B (North Pacific; 51°27.026′N, 168°20.228′E; Fig. 1). Site 884 is located on the flank of Detroit Seamount, at a depth of 3836 m (Shipboard Scientific Party, 1993). Paleobathymetric estimates are based on thermal subsidence and empirical age-depth curves (backtracking technique; e.g., Sclater et al., 1971) and place Site 884 at ~3000–3300 m paleodepth (Pak and Miller, 1995).

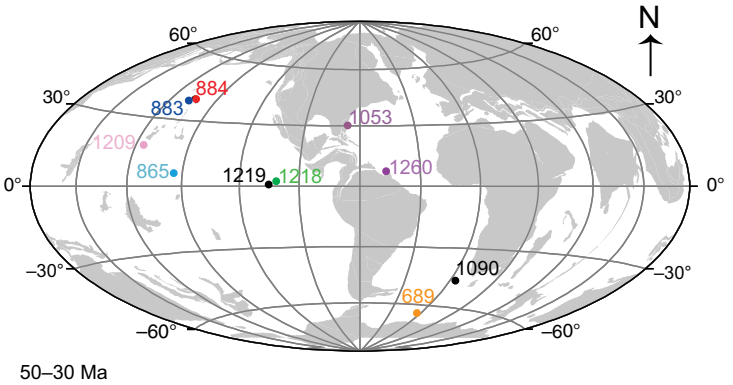


**Figure 1. Paleogeographic reconstruction (50–30 Ma) showing the sites used in this study (Ocean Drilling Stratigraphic Network; http://www.odsn.de). The sites used in the stable isotope intra- and inter-basinal comparisons are color coded. For each site, the color in the map corresponds to the color of the data and trend lines in Figures 5 and 6.**

## Site 884B Age Model

An age model based on biostratigraphic (calcareous nannofossil) datums (Fig. 2; Tables 2–4) was applied to these new stable isotopic records from Site 884B and to the Pak and Miller (1995) records for Site 884B (Figs. 3 and 4). Reworking and mixing of calcareous nannofossil assemblages was documented in some parts of Site 884 sections (Beaufort and Ólafsson, 1995). However, despite some uncertainties in some calcareous nannofossil distributions, several reliable biostratigraphic datums were published (Barron et al., 1995) and used for paleoceanographic reconstructions (Pak and Miller, 1995). Planktonic foraminiferal datums were not used in the age model because there are no planktonic foraminifera in cores 74–81, and planktonic foraminifera are generally rare and poorly preserved in cores 82–84 (Basov, 1995).

Because the biostratigraphic datum ages reported in Berggren et al. (1995) are not well constrained for higher latitude sites in the North Pacific, the biostratigraphic datums used in this study (Table 2) were recalibrated with respect to paleomagnetic datums (Tables 3 and 4; Supplemental Tables 1 and 2, Supplemental Fig. 1, and the Supplemental Information in the Supplemental File[1]). Unfortunately, no magnetostratigraphic data are available for Site 884B from cores 74–84 (Barron et al., 1995), so it was not possible to constrain the calcareous nannofossil datums with a magnetostratigraphic record from Site 884. Because of this, we utilized other sites for the calibration of the biostratigraphic datums used in this study: Site 1053 (western North Atlantic; Shipboard Scientific Party, 1998; Ogg and Bardot, 2001, reinterpreted in Borrelli et al., 2014), Site 1090 (sub-Antarctic South Atlantic; Channell et al., 2003), Site 689 (Southern Ocean; Florindo and Roberts, 2005), and Sites 1218 and 1219 (equatorial Pacific; Pälike et al., 2005) (Fig. 1; Tables 3 and 4; Supplemental Tables 1 and 2 and Supplemental Fig. 1 in the Supplemental File [see footnote 1]). We selected these sites because of their good paleomagnetic records for Eocene sections. First, a site-specific paleomagnetic-based age model was used to determine an age for each biostratigraphic datum at each site. Note that only the biostratigraphic datums reported for Site 884B (Barron et al., 1995), with the exception of HO *Ericsonia formosa* (Shipboard Scientific Party, 1993) (Table 2) were taken into account at each site (Supplemental Tables 1 and 2 and Supplemental Fig. 1 in the Supplemental File [see footnote 1]). Then, for each datum, the age obtained at each site where the datum was calibrated to paleomagnetics was averaged (Tables 3 and 4; Supplemental Tables 1 and 2 and Supplemental Fig. 1 in the Supplemental File [see footnote 1]). Those biostratigraphic datums that

TABLE 1. SUMMARY OF THE SITES USED IN THIS STUDY

| Ocean Drilling Program Site | Basin | Paleodepth (m) | References |
|---|---|---|---|
| 884 | Northwestern Pacific | ~3000–3300 | This study; Shipboard Scientific Party (1993); Barron et al. (1995); Pak and Miller (1995) |
| 883 | Northwestern Pacific | ~1700–2000 | Pak and Miller (1995) |
| 1209 | Subtropical North Pacific | ~1900–2500 | Dutton et al. (2005); Dawber and Tripati (2011) |
| 1218 | Equatorial Pacific | ~3700–4300 | Lear et al. (2004); Coxall et al. (2005); Pälike et al. (2005); Coxall and Wilson (2011) |
| 1219 | Equatorial Pacific | ~3500–4000 | Pälike et al. (2005) |
| 865 | Equatorial Pacific | ~1300–1500 | Bralower et al. (1995) |
| 689 | Southern Ocean | ~1500 | Diester-Haass and Zahn (1996); Bohaty and Zachos (2003); Florindo and Roberts (2005); Bohaty et al. (2012) |
| 1053 | Northwestern Atlantic | ~1500–1700 | Shipboard Scientific Party (1998); Ogg and Bardot (2001); Katz et al. (2011); Borrelli et al. (2014) |
| 1260 | Tropical western Atlantic | ~2500–3200 | Sexton et al. (2006) |
| 1090 | Sub-Antarctic South Atlantic | ~3700 | Channell et al. (2003) |

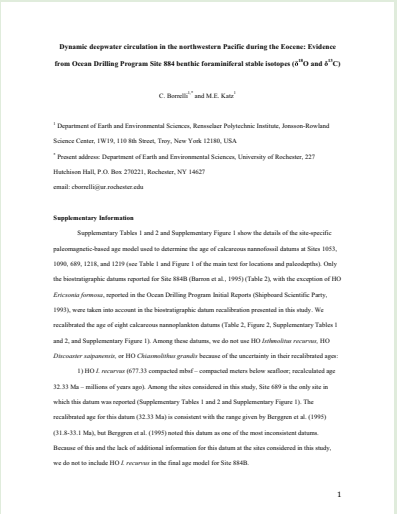

Dynamic deepwater circulation in the northwestern Pacific during the Eocene: Evidence from Ocean Drilling Program Site 884 benthic foraminiferal stable isotopes ($\delta^{18}O$ and $\delta^{13}C$)

C. Borrelli[1,*] and M.E. Katz[1]

[1] Department of Earth and Environmental Sciences, Rensselaer Polytechnic Institute, Jonsson-Rowland Science Center, 1W19, 110 8th Street, Troy, New York 12180, USA

[*] Present address: Department of Earth and Environmental Sciences, University of Rochester, 227 Hutchison Hall, P.O. Box 270221, Rochester, NY 14627

email: cborrelli@ur.rochester.edu

Supplementary Information

Supplementary Tables 1 and 2 and Supplementary Figure 1 show the details of the site-specific paleomagnetic-based age model used to determine the age of calcareous nannofossil datums at Sites 1053, 1090, 689, 1218, and 1219 (see Table 1 and Figure 1 of the main text for locations and paleodepths). Only the biostratigraphic datums reported for Site 884B (Barron et al., 1995) (Table 2), with the exception of HO *Ericsonia formosa*, reported in the Ocean Drilling Program Initial Reports (Shipboard Scientific Party, 1993), were taken into account in the biostratigraphic datum recalibration presented in this study. We recalibrated the age of eight calcareous nannoplankton datums (Table 2, Figure 2, Supplementary Tables 1 and 2, and Supplementary Figure 1). Among these datums, we do not use HO *Isthmolithus recurvus*, HO *Discoaster saipanensis*, or HO *Chiasmolithus grandis* because of the uncertainty in their recalibrated ages:

1) HO *I. recurvus* (677.33 compacted mbsf – compacted meters below seafloor; recalculated age 32.33 Ma – millions of years ago). Among the sites considered in this study, Site 689 is the only site in which this datum was reported (Supplementary Tables 1 and 2 and Supplementary Figure 1). The recalibrated age for this datum (32.33 Ma) is consistent with the range given by Berggren et al. (1995) (31.8–33.1 Ma), but Berggren et al. (1995) noted this datum as one of the most inconsistent datums. Because of this and the lack of additional information for this datum at the sites considered in this study, we do not to include HO *I. recurvus* in the final age model for Site 884B.

1

[1]Supplemental File. 1) Brief description of the calcareous nannofossil datums not included in the final age model of Ocean Drilling Program Site 884, and 2) additional details about the site-specific paleomagnetic-based age model used to determine the age of calcareous nannofossil datums at Ocean Drilling Program Sites 1053, 1090, 689, 1218, and 1219 (Supplemental Tables 1 and 2, and Supplemental Fig. 1). Please visit http://dx.doi.org/10.1130/GES01152.S1 or the full-text article on www.gsapubs.org to view the Supplemental File.

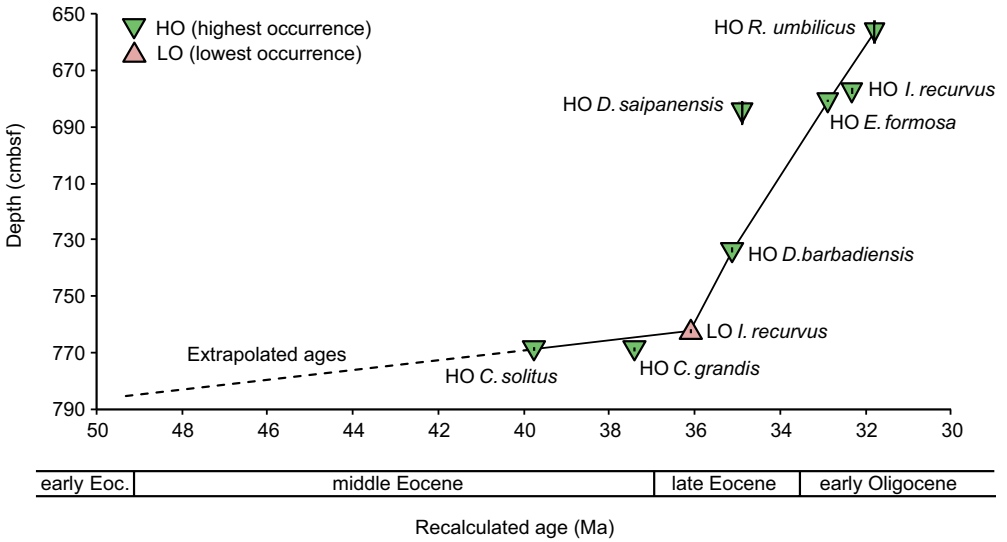


**Figure 2. Age-depth plot showing our age model based on biostratigraphic datums. The ages for samples deeper than HO (highest occurrence) *Chiasmolithus solitus* were extrapolated using LO (lowest occurrence) *Isthmolithus recurvus* and HO *C. solitus* as tie points. Error bars represent the depth range of each datum. (For additional details, see text, Tables 2–4, and the Supplemental File [see footnote 1].) Eoc.—Eocene; cmbsf—compacted meters below seafloor.**

showed the best agreement among the sites used in this calibration (Fig. 2; Tables 2–4) were selected (see the Supplemental Information in the Supplemental File [see footnote 1] for additional discussion of the other nannoplankton datums from Site 884B).

1. HO (highest occurrence) *Reticulofenestra umbilicus* (656.45 compacted mbsf, meters below seafloor; recalculated age 31.80 Ma). This datum is consistent at Sites 1218 and 1219 (32.11 Ma and 32.04 Ma, respectively) (Tables 3 and 4); the upper bounding paleomagnetic C12n/r (chron) reversal is identified at Site 1218 and only the lower C12r-C13n reversal is correlated from Site 1219 (Pälike et al., 2005); it is also consistent with the age in Berggren et al. (1995) of 32.30 Ma at low-middle latitudes. However, this datum at Site 689 is different from the age at Sites 1218 and 1219 (31.23 Ma versus 32.11–32.04 Ma; Tables 3 and 4), even though our recalculated age of HO *R. umbilicus* at Site 689 is in agreement with the calibration of Berggren et al. (1995) of 31.3 Ma at the southern high latitudes.

2. HO *E. formosa* (680.85 compacted mbsf; recalculated age 32.88 Ma). This datum also is consistent at Sites 1218 and 1219 (32.91 Ma and 32.85 Ma, respectively) (Tables 3 and 4), and it is consistent with the datum age of 32.8 Ma reported in Berggren et al. (1995). As for the previous datum, the upper boundary of paleomagnetic C12n/r reversal is identified at Site 1218, and only the lower C12r-C13n reversal is correlated from 1219 (Pälike et al., 2005). This datum is not present at Site 689 (Tables 3 and 4); however, Berggren

TABLE 2. BIOSTRATIGRAPHIC NANNOPLANKTON DATUMS FOR OCEAN DRILLING PROGRAM SITE 884B

| Datum type | Marker | Depth range (compacted mbsf) | Depth (compacted mbsf) | Recalculated age (Ma) | Berggren et al. (1995) age (Ma) | Age offset (m.y.) |
|---|---|---|---|---|---|---|
| HO | ***Reticulofenestra umbilicus*** | **651.70–661.20** | **656.45** | **31.80** | **31.30†–32.30** | **0.50–0.50** |
| HO | *Isthmolithus recurvus* | 676.25–678.40 | 677.33 | 32.33 | 31.80–33.10 | 0.53–0.77 |
| HO | ***Ericsonia formosa**** | **680.60–681.09** | **680.85** | **32.88** | **32.80–39.70†** | **0.08–6.82** |
| HO | *Discoaster saipanensis* | 680.60–689.50 | 685.05 | 34.89 | 34.20–35.40† | 0.69–0.51 |
| HO | ***D. barbadiensis*** | **732.94–734.43** | **733.69** | **35.12** | **34.30–39.00†** | **0.82–3.88** |
| LO | ***I. recurvus*** | **761.70–762.90** | **762.30** | **36.11** | **36.00** | **0.11** |
| HO | *Chiasmolithus grandis* | 768.11–769.14 | 768.63 | 37.43 | 37.10 | 0.33 |
| HO | ***C. solitus*** | **768.11–769.14** | **768.63** | **39.75** | **40.40** | **0.65** |

*Note:* Nannoplankton datums following Barron et al. (1995). HO—highest occurrence; LO—lowest occurrence; mbsf—meters below seafloor. Datums used in this study are in bold.
*From Shipboard Scientific Party (1993).
†Berggren et al. (1995) age for southern high latitudes.

TABLE 3. SUMMARY OF OCEAN DRILLING PROGRAM SITES 1053, 1090, 689, 1218, AND 1219 BIOSTRATIGRAPHIC DATUMS CALCULATED USING A SITE-SPECIFIC PALEOMAGNETIC-BASED AGE MODEL

| Ocean Drilling Program Site | Paleomagnetic datum | Depth* | Age (Ma) | Reference | Calcareous nannoplankton datum | Depth* | Reference | Recalculated age (Ma) |
|---|---|---|---|---|---|---|---|---|
| 1053 | Top C15n | 10.78 | 34.66 | Ogg and Bardot (2001; reinterpreted by Borrelli et al., 2014) | HO *Discoaster barbadiensis* | 9.80 | Shipboard Scientific Party (1998) | 34.57 |
| | Bottom C15n | 19.52 | 34.94 | Ogg and Bardot (2001; reinterpreted by Borrelli et al., 2014) | LO *Isthmolithus recurvus* | 80.73 | Shipboard Scientific Party (1998) | 36.18 |
| | Bottom C17n.1n | 144.83 | 37.47 | Ogg and Bardot (2001; reinterpreted by Borrelli et al., 2014) | | | | |
| 1090 | Top C16n.2n | 296.00 | 35.69 | Channell et al. (2003) | LO *I. recurvus* | 304.51 | Channell et al. (2003) | 36.11 |
| | Bottom C16n.2n | 309.00 | 36.34 | Channell et al. (2003) | | | | |
| 689 | Bottom C12n | 104.90 | 30.94 | Florindo and Roberts (2005) | HO *Reticulofenestra* | 106.54 | Florindo and Roberts (2005) | 31.23 |
| | Top C13n | 116.70 | 33.06 | Florindo and Roberts (2005) | umbilicus | | | |
| | Top C16n.1n | 128.25 | 35.34 | Florindo and Roberts (2005) | LO *I. recurvus* | 132.40 | Florindo and Roberts (2005) | 36.04 |
| | Bottom C16n.2n | 134.20 | 36.34 | Florindo and Roberts (2005) | | | | |
| | Top C18n.1n | 145.60 | 38.43 | Florindo and Roberts (2005) | HO *Chiasmolithus solitus* | 153.14 | Florindo and Roberts (2005) | 39.11 |
| | MECO | 162.86 | 40.00 | minimum $\delta^{18}O$ adjusted to 40 Ma | | | | |
| 1218 | Bottom C12n | 204.67 | 30.94 | Pälike et al. (2005) | HO *R. umbilicus* | 220.85 | Pälike et al. (2005) | 32.11 |
| | Top C13n | 233.88 | 33.06 | Pälike et al. (2005) | HO *Ericsonia formosa* | 231.91 | Pälike et al. (2005) | 32.91 |
| | Bottom C13n | 240.29 | 33.55 | Pälike et al. (2005) | HO *D. barbadiensis* | 245.79 | Pälike et al. (2005) | 34.46 |
| | Top C15n | 246.98 | 34.66 | Pälike et al. (2005) | HO *C. solitus* | 277.82 | Pälike et al. (2005) | 40.39 |
| | Bottom C18n.2n | 273.85 | 40.13 | Pälike et al. (2005) | | | | |
| | Top C19n | 291.08 | 41.26 | Pälike et al. (2005) | | | | |
| 1219 | Bottom C12n | 143.03 | 30.94 | Pälike et al. (2005) | HO *R. umbilicus* | 156.98 | Pälike et al. (2005) | 32.04 |
| | Top C13n | 169.80 | 33.06 | Pälike et al. (2005) | HO *E. formosa* | 167.23 | Pälike et al. (2005) | 32.85 |
| | Top C16n.2n | 182.96 | 35.69 | Pälike et al. (2005) | HO *D. barbadiensis* | 187.22 | Pälike et al. (2005) | 36.32 |
| | Bottom C16n.2n | 187.36 | 36.34 | Pälike et al. (2005) | | | | |

*Note:* Only the datums used in the Site 884 age model are reported in this table. Paleomagnetic ages are from Cande and Kent (1995). HO—highest occurrence; LO—lowest occurrence. C—chron; MECO—middle Eocene climatic optimum. See Figure 1 and Table 1 for locations and paleodepths. See text, Supplementary Tables 1 and 2, and Supplementary Figure 1 (see text footnote 1) for additional details.

*Datum depths: compacted meters below seafloor for Site 1053, meters composite depth for Site 1090, meters below seafloor for Site 689, and revised meters composite depth for Sites 1218 and 1219.

TABLE 4. SUMMARY OF RECALCULATED AGES FOR THE BIOSTRATIGRAPHIC DATUMS USED IN THE AGE MODEL FOR OCEAN DRILLING PROGRAM SITE 884

| Ocean Drilling Program Site | *Reticulofenestra umbilicus* (HO) | *Ericsonia formosa* (HO) | *Discoaster barbadiensis* (HO) | *Isthmolithus recurvus* (LO) | *Chiasmolithus solitus* (HO) |
|---|---|---|---|---|---|
| 1053 | | | 34.57 | 36.18 | |
| 1090 | | | | 36.11 | |
| 689 | 31.23 | | | 36.04 | 39.11 |
| 1218 | 32.11 | 32.91 | 34.46 | | 40.39 |
| 1219 | 32.04 | 32.85 | 36.32 | | |
| Recalculated age | 31.80 | 32.88 | 35.12 | 36.11 | 39.75 |

*Note:* Ages in Ma. HO—highest occurrence; LO—lowest occurrence. The new ages for Site 884 biostratigraphic datums are calculated as the average of the ages for the same biostratigraphic datums at Sites 1053, 1090, 689, 1218, and 1219. We calculate the ages of the biostratigraphic datums at these sites using a site-specific paleomagnetic-based age model (see Table 3). See Figure 1 and Table 1 for locations and paleodepths; see text, Supplementary Tables 1 and 2, and Supplementary Figure 1 (see text footnote 1) for additional details.

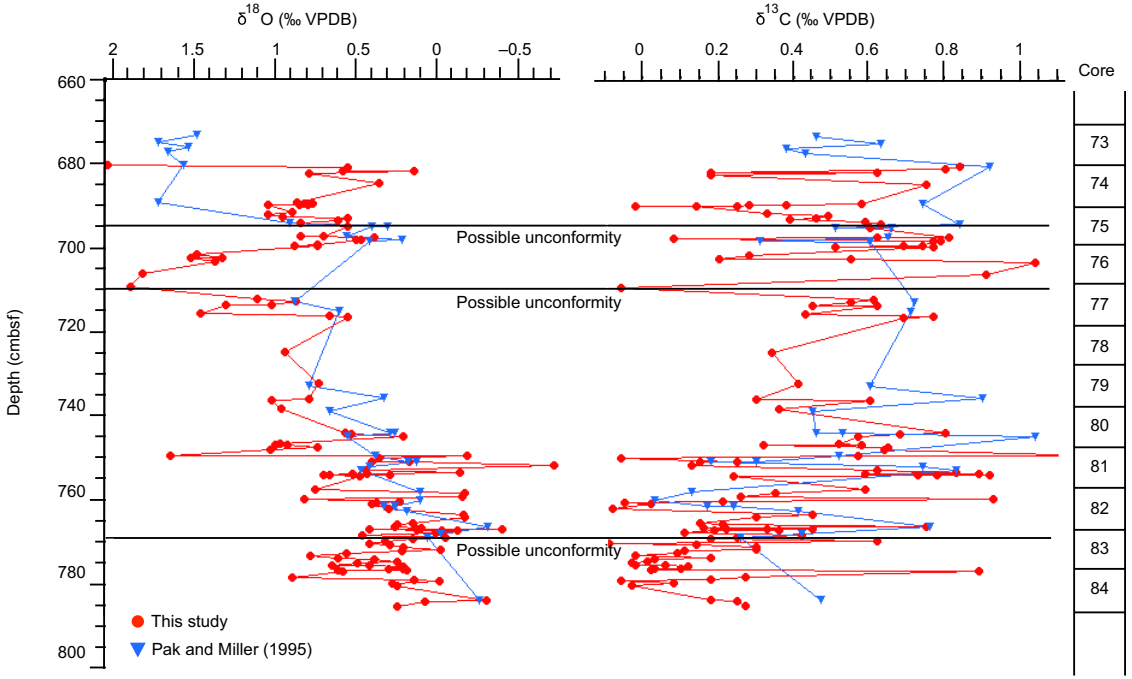


**Figure 3. Benthic foraminiferal stable isotopes ($\delta^{18}O$ and $\delta^{13}C$) versus depth (cmbsf—compacted meters below seafloor) for Ocean Drilling Program Site 884. The depths of three possible unconformities according to Barron et al. (1995) and Pak and Miller (1995) are marked. Site 884 data from this study are plotted together with Site 884 data from Pak and Miller (1995) for comparison. VPDB—Vienna Pee Dee Belemnite.**

et al. (1995) give a very different calibration of HO *E. formosa* for the Southern Ocean (39.7 Ma).

3. HO *Discoaster barbadiensis* (733.69 compacted mbsf; recalculated age 35.12 Ma). This datum is consistent in both the equatorial Pacific (Site 1218, 34.46 Ma; Tables 3 and 4) and the western North Atlantic (Site 1053, 34.57 Ma; Tables 3 and 4), and it is close to the calibration of 34.30 Ma given in Berggren et al. (1995). However, Site 1219 records a much older age for HO *D. barbadiensis* (36.32 Ma; Tables 3 and 4) compared to Site 1218 (34.46 Ma). This datum is not present at Site 689; however, Berggren et al. (1995) assigned an age of 39 Ma to this datum for the Southern Ocean.

4. LO (lowest occurrence) *Isthmolithus recurvus* (762.30 compacted mbsf; recalculated age 36.11 Ma). This datum is consistent at three widespread sites (Sites 1053, 1090, and 689; 36.18 Ma, 36.11 Ma, and 36.04 Ma, respectively; Tables 3 and 4) and is in agreement with the calibration given by Berggren et al. (1995) (36.0 Ma). We note that for the calibration of this datum at Site 1053, we used the paleomagnetic C15 and the lower paleomagnetic C17n.1n because of the uncertainty around the identification of the paleomagnetic C16.2n boundaries (B. Cramer, 2013, personal commun.).

5. HO *Chiasmolithus solitus* (768.63 compacted mbsf; recalculated age 39.75 Ma). The recalibrated datum for Site 1218 (40.39 Ma) is consistent with the age given by Berggren et al. (1995) (40.4 Ma). However, the datum at Site 689 is younger (39.11 Ma) (Tables 3 and 4).

We emphasize that all the nannoplankton biostratigraphic datums selected for the Site 884 age model have a relatively small error (±0.25–0.75 m) due to sample intervals, with the exception of *R. umbilicus* (±4.75 m) (Fig. 2; Table 2). Because it was not possible to recalibrate a calcareous nannofossil datum older than HO *C. solitus,* the age of the samples deeper than 768.63 compacted mbsf (HO *C. solitus*) were extrapolated using LO *I. recurvus* and HO *C. solitus* as tie points (Fig. 2).

Based on this age model (Fig. 2), the sedimentation rate is ~1.74 m/m.y. from the late-middle through the early-late Eocene (similar to the sedimentation rate of ~2.85 m/m.y. recorded at Site 1209; ca. 43–37 Ma) and ~24.56 m/m.y. from the mid-late Eocene through the early Oligocene (see following). As shown here, the isotope correlations between Site 884 and other sites during the middle Eocene climatic optimum (MECO; ca. 39.8–40.6 Ma, Bohaty and Zachos, 2003; Bohaty et al., 2009) support this age model in the older part of the record.

We compare Site 884 to other middle Eocene–early Oligocene benthic foraminiferal stable isotopic records from the Pacific, Atlantic, and Southern Oceans (Fig. 1; Table 1), and provide age model information: (1) ODP Site 883 (northwestern Pacific; ~1700–2000 m paleodepth); (2) ODP Site 1209 (sub-

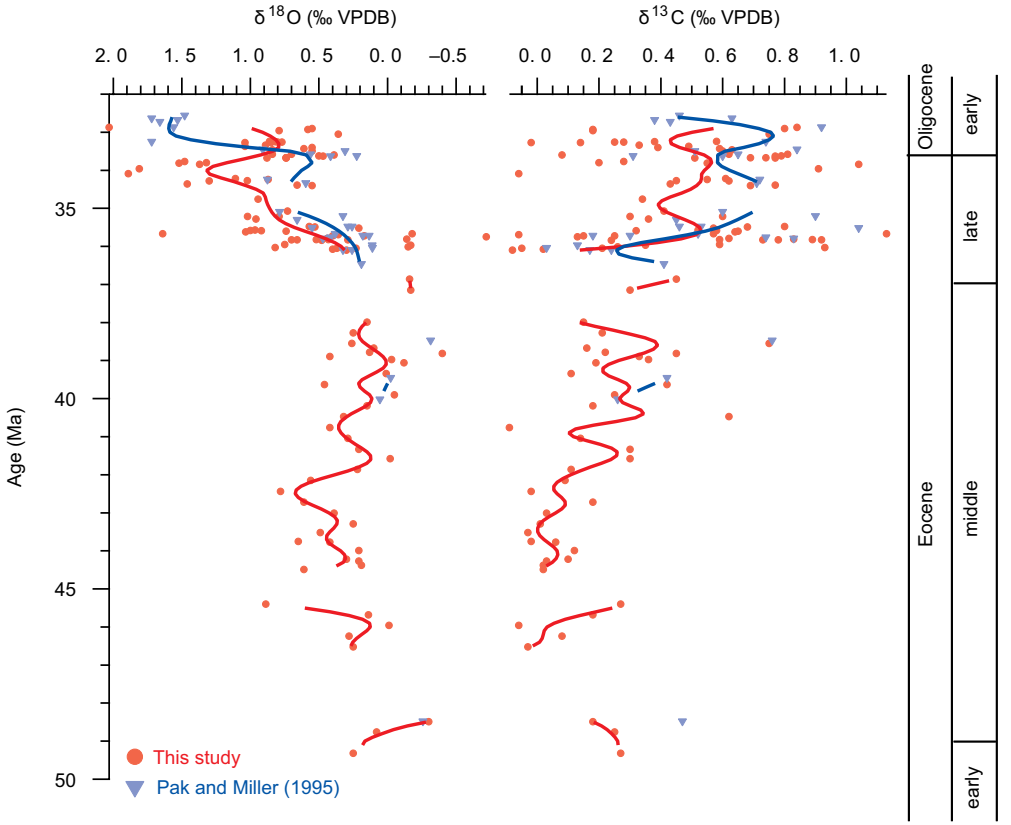


**Figure 4. Benthic foraminiferal stable isotopes ($\delta^{18}O$ and $\delta^{13}C$) versus age (Ma) for Ocean Drilling Program Site 884. Site 884 data from this study are plotted with Site 884 data from Pak and Miller (1995) for comparison. Smooth curves are calculated through a local linear interpolation model, with a resolution of 0.1 m.y. and a width of 1 m.y. Gaps are the result of a low sample resolution in particular intervals of the records. VPDB—Vienna Pee Dee Belemnite.**

tropical North Pacific; ~1900–2500 m paleodepth); (3) ODP Site 1218 (equatorial Pacific; ~3700–4300 m paleodepth); (4) ODP Site 865 (equatorial Pacific; ~1300–1500 m paleodepth); (5) ODP Site 689 (Southern Ocean; ~1500 m paleodepth); (6) ODP Site 1053 (western North Atlantic, ~1500–1700 m paleodepth); and (7) ODP Site 1260 (tropical western Atlantic, ~2500–3200 m paleodepth). All the data points refer to *Cibicidoides* spp. In cases where *Cibicidoides* spp. was not used during isotopic analyses, the data were corrected to *Cibicidoides* spp. using the calibrations of Katz et al. (2003). For each record, the smooth curve was calculated through a local linear interpolation model, with a resolution of 0.1 m.y. and a width of 1 m.y.

Ages from Borrelli et al. (2014) were used for middle Eocene and early Oligocene data from Sites 1218, 1053, 1260, and 689. In addition, ages from Pak and Miller (1995) were used for Site 883, and from Bralower et al. (1995) for Site 865.

Like Site 884, Site 1209 lacks a good magnetostratigraphic record (Shipboard Scientific Party, 2002). For Site 1209, biostratigraphic (calcareous nannofossil) datums from Bralower (2005, bold datums in table 1 therein) were used. For HO *Chiasmolithus grandis* (137.73 rmcd, revised meters composite depth) and HO *C. solitus* (147.16 rmcd), the ages obtained from the datum recalibration described here (37.43 Ma and 39.75, respectively) were used (Table 2; Supplemental Tables 1 and 2 and Supplemental Fig. 1 in the Supplemental File [see footnote 1]). According to our recalibration, HO *C. grandis* is an uncertain datum (additional details are in the Supplemental File [see footnote 1]). Our recalibrated ages for HO *C. grandis* and HO *C. solitus* improve the correlation between Site 1209 and the other sites used in this study.

Note that the ages for all the sites used in this study (Sites 883, 1209, 1218, 865, 689, 1053, and 1260; Fig. 1; Table 1) refer to Berggren et al. (1995) and that the ages for Site 884 (this study) refer to the same magnetostratigraphic time scale (Cande and Kent, 1995). This was done to utilize the biostratigraphic datums tied to this time scale.

### Site 884 Unconformities

Three possible unconformities have been reported in the section analyzed for this study: (1) ~695 mbsf (meters below seafloor, ~695 compacted mbsf), where Barron et al. (1995) identified a possible unconformity at the Eocene-Oligocene boundary according to their age model; (2) ~710 mbsf (~710 compacted mbsf), where Pak and Miller (1995) identified a possible unconformity at the Eocene-Oligocene boundary according to their age model; and (3) ~769 mbsf (~769 compacted mbsf) (Barron et al. 1995). None of these possible unconformities were noted by Hague et al. (2012).

The possible unconformity at ~695 mbsf was identified by Barron et al. (1995) based on sediment redeposition and soft-sediment deformation (Shipboard Scientific Party, 1993), and an abrupt change in sedimentation rate from the Eocene to the Oligocene. However, biostratigraphy does not indicate a hiatus at the Eocene-Oligocene boundary (Barron et al., 1995). Based on benthic foraminiferal reworking and sediment characteristics (e.g., change of color), Pak and Miller (1995) reached a similar conclusion about the possibility of a hiatus at the Eocene-Oligocene boundary (unconformity at ~710 mbsf); however, because of biostratigraphic evidence (the presence of all the biostratigraphic nannofossil zones), Pak and Miller (1995) suggested that if a hiatus were present, it was very brief.

Barron et al. (1995) hypothesized another possible unconformity at ~769 mbsf, at the boundary between lithologic subunit IIB and subunit IIC, as suggested by differences in their lithological and sedimentological features (Shipboard Scientific Party, 1993) and by seismic reflection data (Hamilton, 1995). The age and duration of the associated hiatus match a hiatus recorded at Site 883B (top of the Detroit Seamount, depth 2395 m), suggesting a widespread major change in sedimentation (Barron et al., 1995).

The temporal resolution of this study (~1 k.y. to ~2 m.y.) is not decisive enough to draw firm conclusions about the presence or absence of these unconformities; however, Site 884 benthic foraminiferal stable isotopic data are reasonably constrained around the unconformities at ~769 mbsf (3 samples from this study and 1 sample from Pak and Miller, 1995, between 769.93 and 768.94 compacted mbsf; Fig. 3; Appendix 1) and ~695 mbsf (1 sample from this study and 1 sample from Pak and Miller, 1995).

### Stable Isotope Analyses

Benthic foraminiferal stable isotope ($\delta^{18}O_{bf}$ and $\delta^{13}C_{bf}$) measurements were conducted on 119 Site 884 samples from an ~106 m section, yielding a range of sampling resolution of ~3–846 cm, from cores 74–84, with the lowest sampling frequency from cores 77–80 because of the presence of clay-rich, carbonate-poor samples (Fig. 3). Based on our age model, the samples analyzed spanned ~16.5 m.y. (Fig. 4). Considering the low sampling frequency between cores 77 and 80, the temporal frequency of our samples varies from ~1 k.y. to ~2 m.y. (Appendix 1).

Samples were disaggregated overnight in deionized water or in a sodium metaphosphate and deionized water solution, washed with tapwater through a 63 µm sieve and oven-dried. For stable isotope analyses, monogeneric samples of *Oridorsalis umbonatus*, *Cibicidoides* (*C. eocaenus*, *C. grimsdalei*, *C. havanensis*, *C. praemundulus*, *C. robertsonianus*, *C. subspiratus*), or *Nuttallides truempyi* were selected. The benthic foraminifera were identified using the taxonomy of van Morkhoven et al. (1986) and Miller and Katz (1987). From 1–10 well-preserved tests were ultrasonically cleaned for 2–3 s in order to remove any residual clays prior to the geochemical analyses.

Stable isotope analyses were conducted at the Stable Isotope Laboratory at Rutgers University (New Jersey) using a Micromass Optima mass spectrometer. Samples were reacted with 100% phosphoric acid at 90 °C for 15 min, and calibrated to Vienna Pee Dee Belemnite (VPDB) using an internal standard calibrated against NBS-19. The offset between the internal standard and NBS-19 is ±0.04‰ and ±0.10‰ for $\delta^{18}O$ and $\delta^{13}C$, respectively. Results are reported relative to the VPDB standard. The laboratory standard error (1σ) is ±0.08‰ for $\delta^{18}O$ and ±0.05‰ for $\delta^{13}C$. *Cibicidoides* spp. was preferentially selected for stable isotope analyses. However, specimens of *Oridorsalis* or *Nuttallides* were used as a substitute in 10 samples (this study) that yielded insufficient specimens of *Cibicidoides*. *Oridorsalis* and *Nuttallides* values (this study and Pak and Miller, 1995; Appendix 1) were corrected to *Cibicidoides* using the calibrations of Katz et al. (2003). We did not run replicate analyses because the samples analyzed did not yield enough specimens belonging to the same genus.

## RESULTS

Our new data add substantial detail and structure to the sparse Pak and Miller (1995) data set from ca. 49–33 Ma (cores 73–84; Figs. 3 and 4). Between 50 and 38 Ma, Site 884 recorded $\delta^{18}O_{bf}$ values between ~0.9‰ and ~–0.4‰ and $\delta^{13}C_{bf}$ values between ~–0.1‰ and ~0.7‰ (cores 82–84; Figs. 3 and 4). Beginning ca. 37.5 Ma, the variability of Site 884 $\delta^{18}O_{bf}$ and $\delta^{13}C_{bf}$ increased, with $\delta^{18}O_{bf}$ values between ~2‰ and ~–0.7‰ and $\delta^{13}C_{bf}$ values between ~–0.1‰ and ~1.1‰ (cores 81–74; Figs. 3 and 4).

In order to reconstruct the ocean circulation in the northwestern Pacific from the early Eocene to the earliest Oligocene (ca. 49–33 Ma), the Site 884 $\delta^{18}O_{bf}$ and $\delta^{13}C_{bf}$ records were compared with Sites 883, 865, 1209, 1218, 689, 1260, and 1053 (Figs. 1, 5, and 6; Table 1).

In the late-early Eocene (ca. 49.5 Ma), Site 884 recorded the highest $\delta^{18}O_{bf}$ values among the Pacific locations included in this study (Sites 883, 865, and 1209; Fig. 5). By ca. 46.5 Ma, Site 884 $\delta^{18}O_{bf}$ values became similar to the shallower sites in the northwestern and equatorial Pacific (Sites 883, 865, and 1209; Fig. 5) and tropical Atlantic (Site 1260) (Fig. 6). From ca. 46.5 Ma to ca. 46 Ma, Site 884 $\delta^{18}O_{bf}$ values increased by ~0.5‰ (from ~0.1‰ to ~0.6‰). At the same time, Site 884 recorded low $\delta^{13}C_{bf}$ values (ca. 46 Ma; Figs. 5 and 6). By ca. 45 Ma, Site 884 recorded $\delta^{13}C_{bf}$ values similar to Site 883, whereas other Pacific sites (Sites 865 and 1209; offset between ~0.5‰; Fig. 5), the Atlantic site (Site 1260; offset ~0.6‰; Fig. 6), and the Southern Ocean site (Site 689; offset ~0.4‰; Fig. 6) showed higher $\delta^{13}C_{bf}$ values.

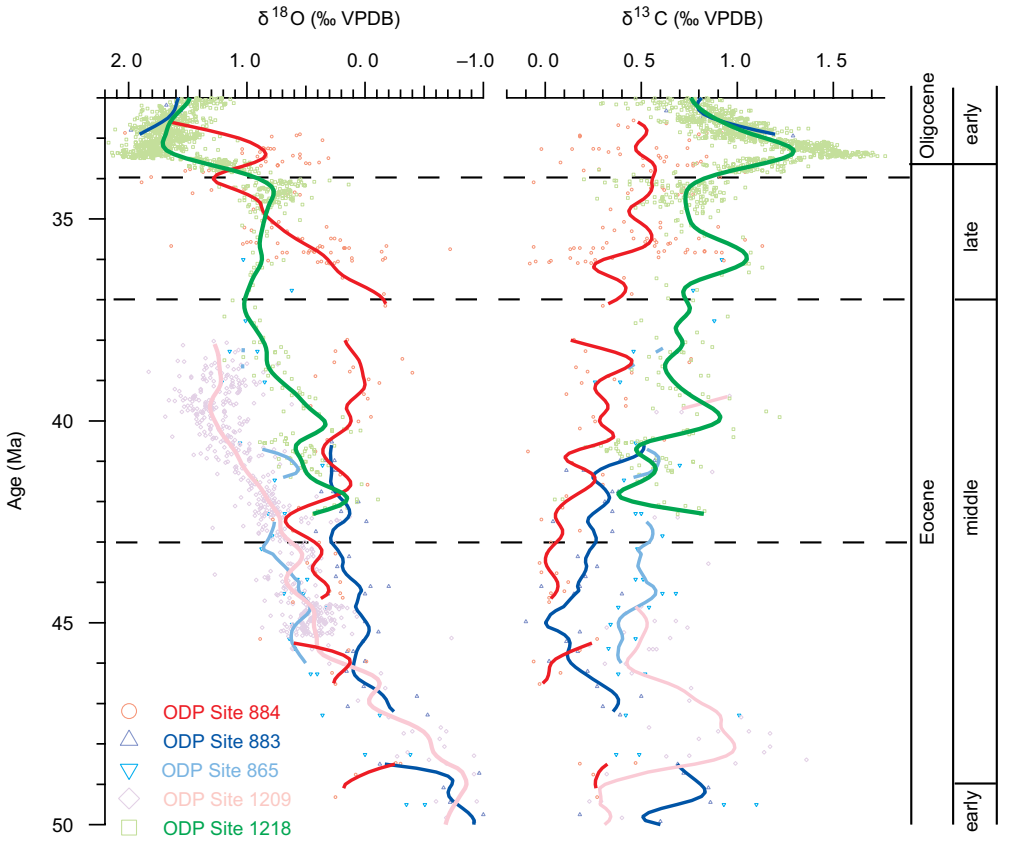


**Figure 5. Comparison among different benthic foraminiferal stable isotope ($\delta^{18}O$ and $\delta^{13}C$) records from several Pacific locations, i.e., Ocean Drilling Program (ODP) Sites 884 (this study and Pak and Miller, 1995), 883 (Pak and Miller, 1995), 865 (Bralower et al., 1995), 1218 (Lear et al., 2004; Coxall et al., 2005; Coxall and Wilson, 2011), and 1209 (Dutton et al., 2005; Dawber and Tripati, 2011). The dashed lines separate the record into the time periods discussed in the text. Smooth curves are calculated through a local linear interpolation model, with a resolution of 0.1 m.y. and a width of 1 m.y. Gaps are the result of a low sample resolution in particular intervals of the records. VPDB—Vienna Pee Dee Belemnite.**

Starting ca. 44.5 Ma, Site 884 $\delta^{18}O_{bf}$ values fluctuate between ~0.7‰ and ~0.3‰. Similar values are recorded also in the subtropical Pacific (ca. 43 Ma; Site 1209), the tropical Atlantic (starting ca. 44 Ma; Site 1260), and the Southern Ocean (starting ca. 44 Ma; Site 689) (Figs. 5 and 6), while the shallower northwestern Pacific (Site 883) records slightly lower $\delta^{18}O_{bf}$ values (ca. 44–43 Ma; offset ~0.3‰) (Fig. 5). At the same time (ca. 44–43 Ma), Site 884 recorded $\delta^{13}C_{bf}$ values ~0‰–0.2‰, similar to the shallower northwestern Pacific Site 883 $\delta^{13}C_{bf}$ values (offset ~0.2‰; Fig. 5), but lower than the subtropical and equatorial Pacific (Sites 865 and 1209), the tropical Atlantic (Site 1260), and the Southern Ocean (starting from ca. 44 Ma; Site 689) (Figs. 5 and 6).

Starting ca. 42 Ma, Site 884 $\delta^{18}O_{bf}$ values become similar to the Site 1218 $\delta^{18}O_{bf}$ values (with a slight offset, ~0.1‰–0.2‰). The $\delta^{18}O_{bf}$ values at both sites decrease ca. 42–41 Ma. A similar trend is recorded at Sites 883 and 865 (Fig. 5), but not at Sites 1209 (Fig. 5), 689, or 1260 (Fig. 6). From the late-middle Eocene (ca. 41 Ma), Site 884 $\delta^{13}C_{bf}$ values decrease, recording the lowest $\delta^{13}C_{bf}$ values (~0.1‰) among the subtropical Pacific sites (Site 1209; Fig. 5), the equatorial Pacific (Site 1218), the Southern Ocean (Site 689), and the tropical Atlantic (Site 1260) (Fig. 6); however, a small and rapid increase in $\delta^{13}C_{bf}$ values and a rapid decrease in $\delta^{18}O_{bf}$, typical of the MECO event (ca. 39.8–40.6 Ma; Bohaty and Zachos, 2003; Bohaty et al., 2009), is evident at Site 884, even if the amplitude of the $\delta^{13}C_{bf}$ shift is much smaller compared do the equatorial Pacific (Site 1218), the Southern Ocean (Site 689), and the Atlantic (Site 1260) (Fig. 6).

From the late-middle until the early-late Eocene (ca. 39–37 Ma), Site 884 $\delta^{18}O_{bf}$ values start to decrease, recording the lowest $\delta^{18}O_{bf}$ values (~–0.2‰) among the North Pacific and equatorial Pacific (Sites 1209, 865, and 1218), the Southern Ocean (Site 689), and the western North Atlantic (Site 1053) (Figs. 5 and 6). In general, from ca. 38–36 Ma, Site 884 $\delta^{13}C_{bf}$ values remain the lowest among the records from the equatorial Pacific (Site 1218, offset ~0.4‰ to ~1.2‰, ca. 37 Ma; Fig. 5), the Southern Ocean (Site 689, offset ~0.4‰ to ~1.3‰, ca. 37 Ma; Fig. 6), and the northwestern Atlantic (Site 1053; offset ~0.8‰; Fig. 6).

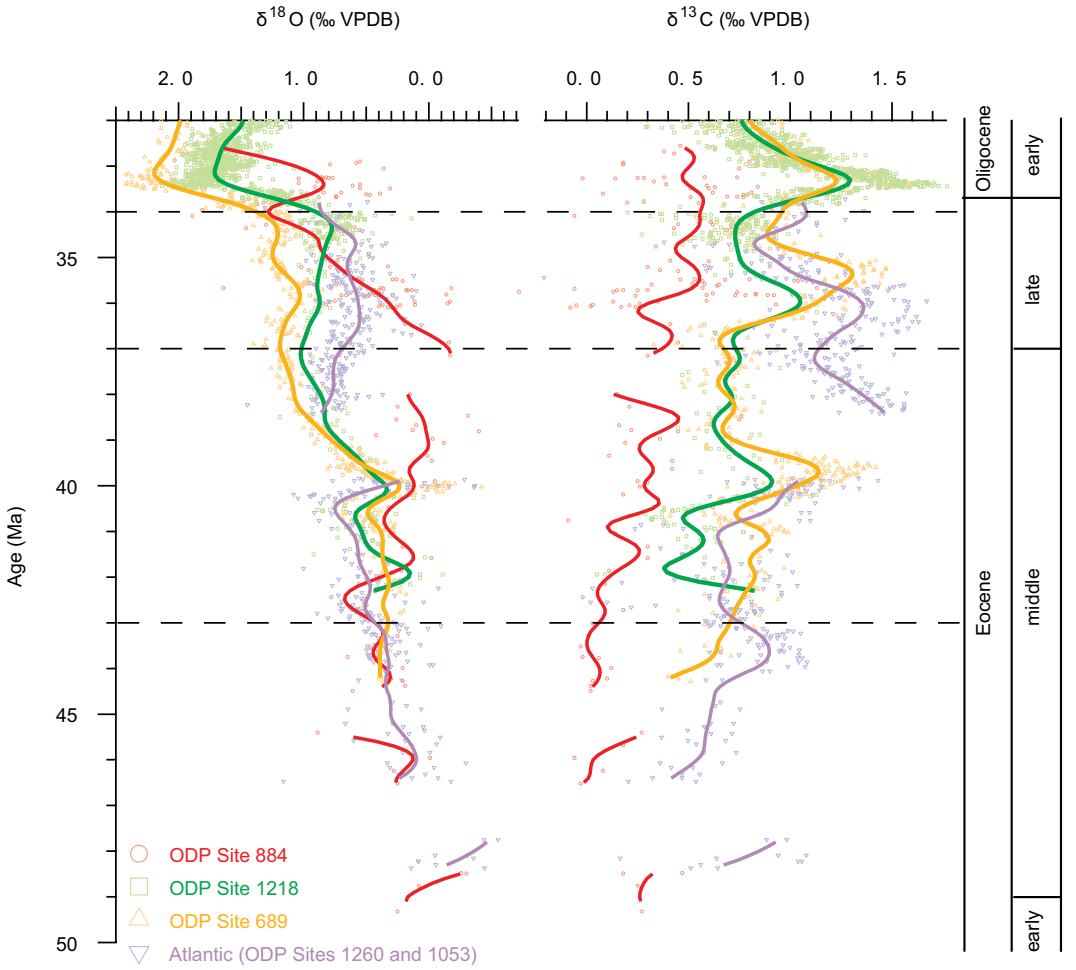


**Figure 6. Comparison among different benthic foraminiferal stable isotope ($\delta^{18}O$ and $\delta^{13}C$) Ocean Drilling Program (ODP) records from the northwestern and equatorial Pacific (Site 884, this study; Pak and Miller, 1995; Site 1218, Lear et al., 2004; Coxall et al., 2005; Coxall and Wilson, 2011), the Southern Ocean (Site 689, Diester-Haass and Zahn, 1996; Bohaty and Zachos, 2003; Bohaty et al., 2012), and the northwestern and western tropical Atlantic (Site 1053, Katz et al., 2011; Borrelli et al., 2014; Site 1260, Sexton et al., 2006). The dashed lines separate the record into the time periods discussed in the text. Smooth curves are calculated through a local linear interpolation model, with a resolution of 0.1 m.y. and a width of 1 m.y. Gaps are the result of a low sample resolution in particular intervals of the records. VPDB—Vienna Pee Dee Belemnite.**

In the late Eocene (ca. 37–34 Ma), Site 884 $\delta^{18}O_{bf}$ and $\delta^{13}C_{bf}$ values start to increase ($\delta^{18}O_{bf}$ reaching ~1.2‰ and $\delta^{13}C_{bf}$ reaching ~0.5‰), becoming more similar to the equatorial Pacific (Site 1218), the Southern Ocean (Site 689), and the western North Atlantic (Site 1053) $\delta^{18}O_{bf}$ and $\delta^{13}C_{bf}$ records (Fig. 6).

In the early Oligocene (ca. 33.5 Ma), Site 884 $\delta^{18}O_{bf}$ values decrease and increase again, reaching values (~1.6‰) similar to the later values recorded at the shallower northwestern and equatorial Pacific (Sites 883 and 1218; Fig. 5), while Site 884 $\delta^{13}C_{bf}$ values remain still lower than in the shallower northwestern (Site 883) and equatorial Pacific (Site 1218) and the Southern Ocean (Site 689) (Figs. 5 and 6).

## Variability of Site 884 $\delta^{18}O_{bf}$ and $\delta^{13}C_{bf}$ Records

Overall, the benthic foraminiferal $\delta^{18}O_{bf}$ and $\delta^{13}C_{bf}$ data collected during this study are in agreement with data from Pak and Miller (1995), with few exceptions (i.e., ~680, 690, 732, 735 and 784 compacted mbsf, Fig. 3; ca. 32.9, 33.3, 35.1, 35.2, and 48.8 Ma, Fig. 4). With the available data, we cannot provide a definitive explanation for the offset between ours and those of Pak and Miller (1995). We note that the data were collected at two different facilities using different instruments. We analyzed our samples at the Stable Isotope Laboratory (Rutgers University) using a Micromass Optima mass spectrometer,

whereas Pak and Miller (1995) analyzed their samples at Lamont-Doherty Earth Observatory (New York) using a Carousel-48 automatic carbonate preparation device attached to a Finnigan MAT 251 mass spectrometer. Therefore, one possible explanation for the offset between our data and the Pak and Miller (1995) data might be related to the instruments and analytical procedures used (e.g., Hönisch et al., 2003; Rosenthal et al., 2004). Alternatively, the offset might be due to differences in the methods used to clean foraminiferal shells (e.g., Rosenthal et al., 2004). We ultrasonically cleaned our samples prior to geochemical analyses; Pak and Miller (1995) ultrasonically cleaned and roasted their samples prior to isotopic analyses. Because the difference between the data is not constant throughout the section analyzed, we think that the previous hypotheses are unlikely. We emphasize that our record has higher resolution compared to the Pak and Miller (1995) record. Because of this, we think that in certain intervals, the Pak and Miller (1995) record missed a variability signal that our record captured. The only exception is the $\delta^{18}O$ samples at ~680 compacted mbsf. Both our record and the Pak and Miller (1995) record have only 1 sample at ~680 compacted mbsf, and the Pak and Miller (1995) sample is in better agreement with the samples at ~677–673 compacted mbsf. In this context, we think that it is possible that our sample might be an outlier.

The Site 884 data show high variability in both $\delta^{18}O_{bf}$ and $\delta^{13}C_{bf}$ (Figs. 3 and 4). The specimens used for isotopic analyses were well preserved and did not show any visible signs of diagenetic alteration, so we exclude the possibility that the Site 884 $\delta^{18}O_{bf}$ and $\delta^{13}C_{bf}$ variability was a consequence of preservational changes of the primary foraminiferal calcite. Variability in both $\delta^{18}O_{bf}$ and $\delta^{13}C_{bf}$ values is not a unique characteristic of Site 884; other sites in different basins recorded high variability during the middle and late Eocene (e.g., subtropical Pacific Site 1209, Dawber and Tripati, 2011; equatorial Pacific Sites 1218 and 1219, Tripati et al., 2005; tropical western Atlantic Sites 1258 and 1260, Sexton et al., 2006; northwestern Atlantic Site 1053, Katz et al., 2011; Borrelli et al., 2014; Atlantic and Indian sector of the Southern Ocean, Sites 689, 738, and 748, Bohaty and Zachos, 2003). Nonetheless, variability is highest at Site 884, and may reflect variable conditions as a consequence of a shift in the deep-water source region and/or mixing of water masses at Site 884; however, because this variability is characteristic of other middle and late Eocene records in different basins, it might be also a consequence of a more general ocean reorganization and climate change. Unfortunately, the temporal resolution of our records is not high enough to draw firm conclusions regarding the variability in $\delta^{18}O_{bf}$ and $\delta^{13}C_{bf}$ values.

## DISCUSSION

### Overview on the Use of $\delta^{18}O_{bf}$ and $\delta^{13}C_{bf}$ to Reconstruct Past Ocean Circulation in the Middle Eocene–Early Oligocene

The $\delta^{18}O_{bf}$ reflects the temperature and the seawater $\delta^{18}O$ signature (as a function of global ice volume) at the time of calcification; however, the influence of these two processes on the $\delta^{18}O_{bf}$ can cancel each other out. For example, in the modern ocean, the $\delta_w$ difference between AABW and NADW is of similar magnitude, but opposite sign, to the temperature difference as measured in $\delta^{18}O_{bf}$ (e.g., Lynch-Stieglitz et al., 1999; Cramer et al., 2011). In Borrelli et al. (2014) it was demonstrated that the $\delta^{18}O_{bf}$ differences between the North Atlantic and Southern Ocean reflected temperature differences between these two deep-water masses in the middle and late Eocene; these conclusions were based on the fact that no realistic ocean circulation mechanism can account for a late Paleogene salinity difference between the North Atlantic and Southern Ocean, equivalent in magnitude but opposite in sign to that characterizing the modern ocean. In addition, modeling simulations showed that ocean circulation would have been driven primarily by thermal rather than salinity differences during the Paleogene (de Boer et al., 2008). As in Borrelli et al. (2014), the Site 884 $\delta^{18}O_{bf}$ signal in the middle and late Eocene is interpreted as only a temperature signal.

The $\delta^{13}C_{bf}$ values are mainly influenced by (1) the $\delta^{13}C_{bf}$ signature of the surface water, which sinks to form deep water; (2) the oxidation of the organic matter sinking from the surface; and (3) mixing among water masses (Kroopnick, 1985). The development of an interbasinal $\delta^{13}C_{bf}$ gradient in the middle and late Eocene was first emphasized in Borrelli et al. (2014); in order to explain this gradient, three scenarios were proposed: (1) variable mixing among deep-water masses (but this was considered unlikely because it would require decoupling between $\delta^{18}O_{bf}$ and $\delta^{13}C_{bf}$ as tracers for deep-water masses); (2) $\delta^{13}C_{bf}$ differences between Northern Component Water (NCW) versus Southern Component Water (SCW) end members, assuming an Eocene $\delta^{13}C_{bf}$ deep-water signature similar to the Neogene; and (3) change in nutrient distribution of surficial water through time. Unfortunately, firm conclusions about the last two scenarios were not drawn because available data were insufficient to test these two hypotheses; however, it was shown (Borrelli et al., 2014) that the use of $\delta^{13}C_{bf}$ values, in conjunction with $\delta^{18}O_{bf}$, was a valid approach to reconstruct past ocean circulation in the middle and late Eocene.

### Modern Ocean Circulation in the Northwestern Pacific

Modern ocean circulation patterns in the northwestern Pacific provide context for our paleocirculation reconstructions. No deep-water formation currently occurs in the North Pacific because of the low salinity characterizing the surface waters of the Subarctic Gyre (Warren, 1983). Because of this low surface salinity, North Pacific Deep Water (NPDW) derives from a different mechanism than NADW, which is composed of different main water sources (i.e., overflows from intermediate depths in the Nordic Seas and Labrador Sea, and water derived from a recirculating AABW [Dickson and Brown, 1994] that join together at the higher latitudes of the North Atlantic before downwelling and flowing south through the Atlantic; e.g., Broecker, 1991; Gordon, 1991). In contrast, NPDW is formed by the vertical mixing of upwelled Pacific Bottom Water (PBW; a blend of NADW and AABW; e.g., Reid and Lynn, 1971; Gordon, 1991) with shallower lower salinity waters reaching deeper depths through mixing processes (e.g., Gordon, 1991).

Part of the mixing process takes place in the Bering Sea (see Scholl et al., 2003, and references therein). A west-running branch of PBW (or NPDW)

flowing north enters the Bering Sea through the Kamchatka Strait after the interaction with bathymetric reliefs and trenches in the northwestern Pacific (i.e., Aleutian Ridge and Kamchatka-Kuril arc trench system); once inside the Bering Sea, this water mass flows eastward and then counterclockwise and mixes with the warmer and more diluted surficial waters of the Bering Gyre (see Scholl et al., 2003, and references therein). This water mass exits the Bering Sea through the western side of the Kamchatka Strait (e.g., Stabeno et al., 1999), blends with PBW, and flows southward following several paths, one of which is east of the Meiji Drift deposit (e.g., Owens and Warren, 2001). Although the deep water bathing the Pacific is the result of mixing processes among different water masses, the detection of anthropogenic cholorofluorocarbons (CFCs) in bottom waters of the Aleutian basin suggests that a small amount of bottom-water formation occurs in the eastern Bering Sea today (Warner and Roden, 1995). The possibility that similar mechanisms might have influenced the middle Eocene ocean circulation in the northwestern Pacific is discussed in the section "Mid-Middle Eocene–Early-Late Eocene $\delta^{18}O_{bf}$ and $\delta^{13}C_{bf}$."

## Ocean Circulation in the Western North Pacific from the Early-Middle Eocene to the Earliest Oligocene

### *Early-Middle Eocene–Mid-Middle Eocene $\delta^{18}O_{bf}$ and $\delta^{13}C_{bf}$*

In the early-middle Eocene (ca. 49–48 Ma) record, Site 884 $\delta^{18}O_{bf}$ values are higher and $\delta^{13}C_{bf}$ values are lower than the shallower northwestern (Site 883) and subtropical (Site 1209) Pacific (Fig. 5). Starting from ca. 47 Ma, Site 884 records $\delta^{18}O_{bf}$ values are similar to those of the equatorial Pacific (Sites 865 and 1209, ca. 47–45 Ma, and Site 1218 starting from ca. 43 Ma; Fig. 5) and the Southern Ocean and the Atlantic (Sites 689 and 1260, starting ca. 45 Ma; Fig. 6). In contrast, $\delta^{13}C_{bf}$ values of Sites 884 and 883 are lower than these other sites (Figs. 5 and 6).

These records are interpreted as evidence of a common water mass (probably originating from different parts of the Southern Ocean) or of different water masses with a similar $\delta^{18}O_{bf}$ signature bathing the northwestern and equatorial Pacific, the Atlantic, and the Southern Ocean at several depths (as suggested by the similar $\delta^{18}O_{bf}$ values among Sites 884, 1218, 689, and 1260; Figs. 5 and 6). Several studies found that the Southern Ocean was an important region of deep-water formation during the early and middle Eocene (e.g., Pak and Miller, 1995; Via and Thomas, 2006; Thomas et al., 2008; Hague et al., 2012); however, neodymium isotope data indicate the presence of deep convection in the North Pacific as well (e.g., Hague et al., 2012). Regardless of the origin of the deep-water masses flowing at different sites, the similarity among $\delta^{18}O_{bf}$ values from Pacific, Atlantic, and Southern Ocean sites located at several paleodepths (Figs. 5 and 6; Table 1) suggests that the thermal structure of the oceans was quite homogeneous from the early-middle until the mid-middle Eocene (as noted by Pak and Miller, 1995; Cramer et al., 2009). This observation is supported by modeling experiments that suggest a homogeneous deep thermal structure of the oceans in the absence of the ACC (Cox, 1989; Toggweiler and Samuels, 1998; Toggweiler and Bjornsson, 2000). An interesting exception is Site 883, which recorded $\delta^{18}O_{bf}$ values ~0.5‰ lower than Site 884 $\delta^{18}O_{bf}$ values. The agreement between the benthic foraminiferal stable isotope records at Site 883 and nearby Site 577 in intervals of overlap suggests that diagenesis did not significantly affect the Site 883 $\delta^{18}O_{bf}$ values (Pak and Miller, 1995). One possible explanation for the low $\delta^{18}O_{bf}$ values at Site 883 might be the presence of a different, warmer, and possibly regional deep-water mass flowing at this site. Based on neodymium isotopes, Hague et al. (2012) proposed a water mass that originated from the North Pacific and affected the northernmost sites of the Pacific ca. 45 Ma. Site 883 recorded relatively low $\delta^{13}C_{bf}$ values, more similar to the Site 884 $\delta^{13}C_{bf}$ values than to other Pacific sites (Fig. 5). The similarity of $\delta^{18}O_{bf}$ values among Site 884 and other locations in different basins (Figs. 5 and 6) supports the hypothesis that Site 884 was bathed by a deep-water mass that originated in the Southern Ocean or by a water mass with a $\delta^{18}O_{bf}$ isotopic signature similar to those bathing the other sites considered in this study. In this scenario, the relatively low $\delta^{13}C_{bf}$ values recorded at Site 884 could be the consequence of an accumulation of old water in the deep North Pacific, as occurs today (Kroopnick, 1985). However, if Site 883 was bathed by a deep-water mass that originated in the North Pacific (Hague et al., 2012), the Site 883 $\delta^{13}C_{bf}$ values could be the consequence of nutrient-rich waters that downwelled from the surface in the northernmost Pacific (Cramer et al., 2009).

This assertion reveals a more complicated ocean structure than the Pak and Miller (1995) reconstruction for the ocean circulation in the northwestern Pacific from ca. 49 to 43 Ma. Pak and Miller (1995) proposed that the deep water that originated in the Southern Ocean was the single dominant water mass bathing the northwestern Pacific in the early-middle Eocene. However, the intrabasinal and interbasinal comparisons presented in this study reveal that at least two water masses bathed the Pacific at that time: one water mass (or different water masses with similar $\delta^{18}O_{bf}$ signature) bathing the Southern Ocean (Site 689), the Atlantic (Site 1260), and the equatorial (Sites 865, 1209, and 1218) and deep northwestern (Site 884) Pacific, and a water mass with a distinctive $\delta^{18}O_{bf}$ signature bathing the shallow northwestern Pacific (Site 883).

### *Mid-Middle Eocene–Early-Late Eocene $\delta^{18}O_{bf}$ and $\delta^{13}C_{bf}$*

Beginning ca. 42 Ma, Site 884 started to record $\delta^{18}O_{bf}$ values similar to Site 883 $\delta^{18}O_{bf}$ values. These relatively low $\delta^{18}O_{bf}$ values (~0.2‰ to –0.2‰; Figs. 5 and 6) characterize the Site 884 record until 37 Ma. In this study, Eocene $\delta^{18}O_{bf}$ values are interpreted as a temperature signal, so the Site 884 $\delta^{18}O_{bf}$ values indicate a warm deep-water mass at Site 884. Based on the Site 884 $\delta^{13}C_{bf}$ values, there are two possible scenarios for the origin of the warm water mass at Site 884 at that time: (1) downwelling of a nutrient-rich deep-water mass at the higher latitudes of the North Pacific (e.g., Bering Sea; Scholl et al., 2003), or (2) the accumulation of warm and saline deep water originating from mid-latitudes, possibly the Tethys (Pak and Miller, 1995).

Modeling experiments show that surface water sinking in the North Pacific is possible only under specific conditions. In a warm ocean, such as in

the late Paleogene, the ocean overturning circulation would have been driven primarily by thermal rather than salinity differences, possibly allowing convection in the North Pacific (de Boer et al., 2008). According to this model, the hydrologic cycle played a minor role in driving the meridional overturning circulation. However, as simulated by Saenko et al. (2004) and Menviel et al. (2012), freshwater perturbations (in particular, a negative freshwater flux in the North Pacific or a positive freshwater flux in the North Atlantic) might drive the formation of deep water in the North Pacific, even with a closed Bering Strait, a condition similar to the middle Eocene–early Oligocene (e.g., Sempson, 1947; Hopkins, 1959). In addition, paleoceanographic reconstructions show that there was no significant change in depth or topography of the Panama gateway until the middle and late Miocene (Haug and Tiedmann, 1998; Martin and Haley, 2000). An open Panama gateway could have reduced the salinity contrast between the Atlantic and the Pacific waters (as modeled by Lunt et al., 2008) and could have allowed a deep convection in the North Pacific reaching depths of 2000 m (as modeled by Motoi et al., 2005).

Paleoceanographic reconstructions using neodymium isotopic ratios ($\varepsilon_{Nd}$) from the northern (Deep Sea Drilling Project [DSDP] Site 192, ODP Sites 883 and 884), subtropical (ODP Sites 1209 and 1211), central (DSDP Sites 464 and 465), and equatorial (ODP Site 1215) Pacific suggest that deep-water formation in the North Pacific occurred from the late-early until the mid-middle Eocene (ca. 50–45 Ma) (Thomas, 2004; Thomas et al., 2008; Hague et al., 2012). In addition, neodymium isotope data from the equatorial Pacific (Sites 1217, 1219, and 1221) suggest the presence of a second deep-water mass that likely originated from the Southern Ocean (Thomas et al., 2008). According to this reconstruction, the Pacific was characterized by a bipolar ocean circulation until ca. 40 Ma, when the ocean circulation in the northern subtropical Pacific (Sites 1209 and 1211) switched back to a deep-water mass that originated from the Southern Ocean ca. 40 Ma (Thomas, 2004). Hague et al. (2012) noted that Site 884 recorded relatively high radiogenic $\varepsilon_{Nd}$ values in the late Eocene, but they did not draw any conclusions about the reason for these radiogenic values in the northernmost Pacific at that time. It is interesting to note that Site 1218 recorded intermediate $\delta^{18}O_{bf}$ values between Sites 1209 and 884 (Fig. 5). Neodymium isotopes at the equatorial Pacific Sites 1215, 1217, 1219, and 1221 exclude Atlantic deep-water flow through the Caribbean gateway to these sites (Thomas et al., 2008). Because of this, the offset of $\delta^{18}O_{bf}$ values between Sites 1209 and 1218 cannot be explained by a mixing of deep-water masses originating from the Southern Ocean and Atlantic at Site 1218. A possible speculation is that Site 1218 was the location of mixing between deep water that originated in the Southern Ocean and the deep-water mass bathing Site 884; however, $\varepsilon_{Nd}$ values recorded at Site 1219 suggest only the Southern Ocean as the deep-water source region for the equatorial Pacific after ca. 42 Ma (Thomas et al., 2008).

The Site 884 record reveals increasing complexity in deep-water circulation with a change in the source region of the deep-water bathing this site from the mid-middle to the early-late Eocene. Scholl et al. (2003) proposed two scenarios for possible thermohaline circulation in the northern Pacific in order to explain the causes of the formation of the Meiji Drift, a sedimentary belt that began to form in the early Oligocene (e.g., Rea et al., 1995), possibly as a consequence of a thermohaline deep-ocean current in the North Pacific (Mammerickx, 1985). (1) Thermohaline circulation originated in the Bering Sea. In the early and middle Tertiary, it is likely that the southwestern side of the Bering Sea was more open than today to paths of deep-water circulation (Scholl et al., 2003). In this scenario, relatively warm and salty subtropical Pacific waters could have entered the Bering Sea, where, as a consequence of the Oligocene global cooling, these waters could have become sufficiently cold and dense to sink to abyssal depths and flow west of the Aleutian Ridge (through several deep passages). (2) Thermohaline circulation originated outside the Bering Sea. In this scenario, bottom waters coming from other basins (North Atlantic and Southern Ocean) and entering the Bering Sea along the Pacific side of the Kamchatka Trench could have driven northern and western boundary currents to flow counterclockwise before exiting the basin along the eastern side of Shirshov Ridge or the basin's Kamchatka margin (Scholl et al., 2003). This last scenario seems a less likely explanation for the Site 884 record because of the absence of a deep western boundary current between ca. 40 and 36 Ma (e.g., Carter et al., 2004; Thomas et al., 2008). Although not mentioned by Scholl et al. (2003), we think that the Pak and Miller (1995) hypothesis of a mid-latitude deep-water mass bathing Site 884 can be considered as another scenario for thermohaline circulation originated outside the Bering Sea.

Site 884 $\delta^{18}O_{bf}$ and $\delta^{13}C_{bf}$ from the late-middle Eocene to the early-late Eocene might be interpreted as indicating the presence of a nutrient-rich deep-water mass at the higher latitudes of the North Pacific (e.g., Bering Sea; Scholl et al., 2003) or as the presence of old warm waters originating at low latitudes (as proposed by Pak and Miller, 1995). From the record collected for this study, it is difficult to constrain the source region of the deep-water flowing at Site 884 from ca. 40 to ca. 37 Ma. However, because Site 884 records the lowest $\delta^{18}O_{bf}$ values of the Pacific, Atlantic, and Southern Ocean, it is likely that the deep-water mass bathing the northwestern Pacific at ~3000 m originated in the northern Pacific and was not part of a more global ocean circulation route. In the mid-late to early-late Eocene, it is possible that the water mass at Site 884 originated in the Bering Sea from the cooling and sinking of relatively warm and salty subtropical surface waters (scenario 1). Once downwelled, this deep-water mass moved from the Bering Sea southeastward at deep depths (~3000 m) through the Kamchatka Strait, as supported by middle and late Eocene Site 884 $\delta^{13}C_{bf}$ values. This interpretation is not in conflict with the lack of a drift deposit in the North Pacific during the late-middle and early-late Eocene. It is not known whether a local or distal deep-water source was responsible for the formation of the Meiji Drift deposit (Scholl et al., 2003). It is possible that the late-middle Eocene–early-late Eocene deep-water source region for Site 884 was different from the one responsible for the initiation of the Meiji Drift and/or that this circulation was not vigorous enough to initiate the formation of a sedimentary drift.

The possibility that deep water might have formed in the North Pacific from the mid-middle to the early-late Eocene is in agreement with modeling simulations (de Boer et al., 2008) that show possible convection in the North Pacific when the ocean was dominated by thermal rather than salinity differences. In addition, the possibility of a North Pacific–sourced deep-water mass is sup-

ported by relatively radiogenic $\varepsilon_{Nd}$ values recorded in the northwestern Pacific at the time (Sites 883 and 884; Hague et al., 2012). This interpretation agrees with the presence (but not on the source region) of a warm deep-water mass at Site 884 proposed by Pak and Miller (1995), although in this case the timing is different: Pak and Miller (1995) proposed the presence of this deep-water mass from the late Eocene until the Oligocene (ca. 36.46–32.56 Ma; ages are according to the age model used in this study), whereas the higher resolution data of this study compared with additional published records not yet available in 1995 (Sites 1209, 1218, 689, 1053, and 1260) indicate the presence of a warm deep-water mass bathing Site 884 ca. 40–37 Ma.

The possibility that deep-water might have formed in the North Pacific from the mid-middle to the early-late Eocene does not agree with the conclusions reached by Thomas (2004) and Thomas et al. (2008) of deep-water formation in the North Pacific from the late-early to the mid-middle Eocene (ca. 50–45 Ma). However, these studies were based on sites shallower than Site 884 (e.g., Site 1209, paleodepth ~2400 m; Site 1211, paleodepth ~2900 m [Thomas, 2004] versus Site 884 ~3000–3300 m paleodepth), with the exception of Site 1215 (paleodepth ~3600 m; Thomas et al., 2008) that might have been located at the southern limit of this North Pacific deep-water mass ca. 50–49 Ma (Thomas et al., 2008). The interpretation of the Site 884 record does not exclude the presence of a deep-water mass originating in the North Pacific at that time; however, it excludes that this water influenced Site 884 before ca. 40 Ma.

### *Mid-Late Eocene–Late-Late Eocene $\delta^{18}O_{bf}$ and $\delta^{13}C_{bf}$*

A change in deep-water circulation ca. 36.5 Ma is indicated by Site 884 $\delta^{18}O_{bf}$ values, which became similar to those of Sites 1053 and 1218 (northwestern Atlantic and equatorial Pacific, respectively) (Fig. 6). In addition, this change was coeval with the shift of Site 884 $\delta^{13}C_{bf}$ values toward those of Sites 1218, 689, and 1053 (Fig. 6). This is interpreted as evidence that deep water originating from the Southern Ocean reached Site 884. It is possible that this change was related to tectonic movements that opened key Southern Ocean gateways: (1) the Drake Passage (ca. 41 Ma; Scher and Martin, 2006; Livermore et al., 2007) and (2) the Tasman Rise (starting before 35.5 Ma; Exon et al., 2004; Stickley et al., 2004), possibly as early as 50–49 Ma (Bijl et al., 2013), allowing for the development of a proto–ACC (defined as a current around Antarctica, shallower than the modern current because of the more constricted Drake and Tasman gateways; Borrelli et al., 2014).

Benthic foraminiferal stable isotope reconstructions showed that a current around Antarctica affected the deep-water circulation in the Northern Atlantic in the middle and late Eocene and early Oligocene (Katz et al., 2011; Borrelli et al., 2014). Similarly, the evolution of the ACC may also have affected ocean circulation in the northwestern Pacific, with Site 884 being bathed by a different deep-water mass compared to the mid-middle and early-late Eocene. This hypothesis is supported by neodymium reconstructions. Thomas et al. (2008) noted a decreasing trend in $\varepsilon_{Nd}$ values in the subtropical and equatorial Pacific starting ca. 36 Ma; they interpreted this signal as the possible evidence of a deep western boundary current reaching the Pacific from the Southern Ocean after the opening of the Tasman gateway (following Stickley et al., 2004). van der Flierdt et al. (2004) reached a similar conclusion based on the Nd and Pb isotope composition of three ferromanganese crusts in the South Pacific, even though they proposed the beginning of the export of deep water from the Southern Ocean to the Pacific at the Eocene-Oligocene boundary, as also indicated by sedimentary features (e.g., erosion), which began to develop off eastern New Zealand in the early Oligocene (Carter et al., 2004).

### *Eocene-Oligocene Boundary and Earliest Oligocene $\delta^{18}O_{bf}$ and $\delta^{13}C_{bf}$*

Site 884 is the only site among the ones considered in this study (Fig. 1; Table 1) that recorded a decrease in $\delta^{18}O_{bf}$ at the Eocene-Oligocene boundary and in the earliest Oligocene (ca. 33.7–33.3 Ma). We note that the $\delta^{18}O_{bf}$ and $\delta^{13}C_{bf}$ trends of our study and those of Pak and Miller (1995) are opposite between ca. 34.5 and 33 Ma (cores 77–74; Figs. 3 and 4); however, there is a general agreement between our data values and the Pak and Miller (1995) data, even though our data are higher resolution and have a higher variability. In addition, our data set does not include data younger than ca. 32.9 Ma, whereas the Pak and Miller (1995) record includes 5 samples between ca. 32.9 and 32.6 Ma. The smooth curves (trends) were calculated through a local linear interpolation model, with a resolution of 0.1 m.y. and a width of 1 m.y. Such values were selected taking into account the variability and distribution of our data points; however, because of the difference in sample variability and distribution between our record and the Pak and Miller (1995) record ca. 34.5–33 Ma, the calculated trends are opposite ca. 34.5–33 Ma.

As identified by Barron et al. (1995) and suggested by Pak and Miller (1995), a hiatus may be present at Site 884 the Eocene-Oligocene boundary (~695 compacted mbsf; Barron et al., 1995; or ~710 compacted mbsf; Pak and Miller, 1995); however, biostratigraphy does not seem to support this hypothesis (see Material and Methods discussion).

Uncertainties in the age model may be a possible reason for the low $\delta^{18}O_{bf}$ values recorded at Site 884; however, the interval 35.12–32.89 Ma is constrained by reliable calcareous nannoplankton datums from the middle Eocene to the early Oligocene: the HO *E. formosa* (a datum also used by Pak and Miller, 1995) and *D. barbadiensis* (Table 1). The recalculated age for the HO *E. formosa* (32.88 Ma) is consistent at both Sites 1218 and 1219, and it is in good agreement with this datum age of 32.8 Ma reported in Berggren et al. (1995); the recalculated age for the HO *D. barbadiensis* (35.12 Ma) is consistent at both Sites 1218 and 1053 and it is reasonably close to the datum age of 34.30 given in Berggren et al. (1995) (see Material and Methods discussion). Another possible explanation is downslope transport that redeposited middle Eocene sediment at the top of the upper Eocene section at Site 884. This scenario is supported by the Site 884 core 74 description (Rea et al., 1993); however, no signs of debris flow deposit are reported for cores 75–76 (Rea et al., 1993), and $\delta^{18}O_{bf}$ values recovered from the samples of this core are in general agreement with the $\delta^{18}O_{bf}$ values from core 74 samples (Appendix 1).

Following Borrelli et al. (2014), we interpret the Eocene $\delta^{18}O_{bf}$ signal as a temperature signal; however, interpreting the early Oligocene $\delta^{18}O_{bf}$ values only in terms of temperature is incorrect because of the changes in $\delta_w$ as consequence of ice-sheet buildup at the Eocene-Oligocene boundary–earliest Oligocene (e.g., Miller and Fairbanks, 1985; Zachos et al., 1992; Coxall et al., 2005; Katz et al., 2008; Lear et al., 2008). If we assume that the age model is well constrained for the late Eocene–early Oligocene and that downslope transport did not affect cores 75 and 76, it would be reasonable to assume that the $\delta^{18}O_{bf}$ decrease recorded at Site 884 is a real signal, possibly reflecting a temperature component.

Using Mg/Ca data, Lear et al. (2000) proposed that the early Oligocene continental-scale ice accumulation was not associated with a decrease in deep-water temperature. In addition, based on benthic foraminiferal Mg/Ca data, Lear et al. (2004) proposed a 2 °C warming of deep-water at Site 1218 during oxygen isotope event 1 (Oi-1), 33.54 Ma (e.g., Zachos et al., 1996; Katz et al., 2008; Miller et al., 2008b). Lear et al. (2004) suggested two possible explanations for this signal: (1) a real temperature increase, due to a negative feedback of ice buildup in Antarctica (increase in atmospheric carbon dioxide due to reduced chemical weathering of the Antarctic silicate bedrock); or (2) a carbonate saturation effect on benthic foraminiferal Mg/Ca. Even though Pearson et al. (2009) demonstrated that an increase of atmospheric carbon dioxide levels in the atmosphere occurred in the earliest Oligocene, it is unlikely that there was an early Oligocene deep-water warming due to a negative feedback consequent to Antarctica glaciation (cf. Pusz et al., 2011) because (1) the magnitude of the warming described by Lear et al. (2004) would require the accumulation of an ice volume bigger than the modern Antarctica ice budget (e.g., Coxall et al., 2005); (2) modeling simulations suggested that Northern Hemisphere glaciation at the Eocene-Oligocene transition was unlikely (DeConto et al., 2008), even though some studies hypothesized the presence of ice sheets in the Northern Hemisphere in the early Oligocene (Coxall et al., 2005; Tripati et al., 2005); and (3) recent studies show that changes in the carbonate ion concentration and saturation state can mask the influence of temperature on the benthic foraminiferal Mg/Ca ratio (e.g., Elderfield et al., 2006; Rosenthal et al., 2006; Yu and Elderfield, 2008; Pusz et al., 2011). Unfortunately, considering the available data and temporal resolution of this record, we cannot provide a conclusive explanation for the Site 884 decrease in $\delta^{18}O_{bf}$ values ca. 33.7–33.3 Ma. Additional benthic foraminiferal stable isotope data from Site 884 and from other deep-water sites in the northwestern Pacific, possibly together with Mg/Ca data from these same sites, are needed in order to better explain what caused the anomalous, relatively low $\delta^{18}O_{bf}$ values at Site 884 during this time period and to draw a firm conclusion about the Site 884 record at the Eocene-Oligocene boundary and in the earliest Oligocene.

## CONCLUSIONS

In this study we investigated the ODP Site 884 $\delta^{18}O_{bf}$ and $\delta^{13}C_{bf}$ records in order to reconstruct the ocean circulation in the northwestern Pacific from the middle Eocene to the early Oligocene (Table 5). These records add sig-

TABLE 5. SUMMARY OF THE RESULTS AND INTERPRETATIONS OF THIS STUDY

| Time interval (Ma) | Paleoceanographic interpretation of the ODP Site 884 record | Main evidence |
|---|---|---|
| Eocene-Oligocene boundary to earliest Oligocene (ca. 33.7–33.3 Ma) | Sediment redeposition, age model issue, real signal? | Relatively low ODP Site 884 $\delta^{18}O_{bf}$ values |
| mid-late Eocene to late-late Eocene (ca. 36.5–34 Ma) | Water mass likely originated from the Southern Ocean | Increased similarity of the ODP Site 884 $\delta^{18}O_{bf}$ and $\delta^{13}C_{bf}$ values with published $\delta^{18}O_{bf}$ and $\delta^{13}C_{bf}$ records from the Pacific, Atlantic, and Southern Oceans |
| mid-middle Eocene to early-late Eocene (ca. 42–37 Ma) | Local water mass at Site 884, with 2 possible sources: (1) nutrient-rich surface waters downwelling at the higher latitudes of the North Pacific (Bering Sea); or (2) warm saline deep waters originating at low latitudes (possibly from the Tethys) | Relatively low ODP Site 884 $\delta^{18}O_{bf}$ and $\delta^{13}C_{bf}$ values; dissimilarities with other $\delta^{18}O_{bf}$ and $\delta^{13}C_{bf}$ published records from the Pacific, Atlantic, and Southern Oceans |
| Early-middle Eocene to mid-middle Eocene (ca. 49–43 Ma) | Site 884 was bathed by a water mass that likely originated from the Southern Ocean, or by a water mass having a $\delta^{18}O_{bf}$ signature similar to those of the water masses bathing the northwestern and equatorial Pacific, the Atlantic, and the Southern Oceans across a range of paleodepths. | Similarity of ODP Site 884 $\delta^{18}O_{bf}$ values with published $\delta^{18}O_{bf}$ records from the Pacific, Atlantic, and Southern Oceans |

*Note:* ODP—Ocean Drilling Program; bf—benthic foraminiferal.

nificant structure to a lower resolution record by Pak and Miller (1995) and show that the ocean circulation in the northwestern Pacific was very dynamic from ca. 49 to ca. 33 Ma. In particular, the Site 884 $\delta^{18}O_{bf}$ and $\delta^{13}C_{bf}$ data indicate that the northwestern Pacific was bathed by three different deep-water masses from the early-middle Eocene to the early Oligocene: (1) a water mass probably originating from the Southern Ocean or having a $\delta^{18}O_{bf}$ signature similar to that of the water masses bathing the northwestern and equatorial Pacific, the Atlantic, and the Southern Oceans across a range of paleodepths (ca. 49 to ca. 43 Ma); (2) a water mass originating from downwelling of nutrient-rich surface waters at the higher latitudes of the North Pacific (Bering Sea) or warm saline deep waters originating at low latitudes (possibly from the Tethys) (ca. 42 to ca. 37 Ma); and (3) a water mass originating from the Southern Ocean (ca. 36.5–34 Ma). We speculate that this last change in ocean circulation in the northwestern Pacific was linked to the opening of ocean gateways (Drake Passage and Tasman Rise) and ACC development, but further investigation of high-latitude sites in the northern Pacific is needed to firmly establish this link.

**ACKNOWLEDGMENTS**

This research was supported by National Science Foundation (NSF) grant OCE-09-28607/09-27663 (Miriam E. Katz and Benjamin S. Cramer). We are grateful to Ben Cramer (Theiss Research, Eugene, Oregon) for insights on the biostratigraphic datum recalibration, helpful comments during the preparation of this manuscript, and for sharing his data analysis software and the files containing all the benthic foraminiferal stable isotope data used in our intrabasinal and interbasinal comparison. Borrelli thanks Brianna King and Hannah Smith (Rensselaer Polytechnic Institute) for washing the Site 884B samples and Richard Mortlock and James Wright (Rutgers University, New Jersey) for their help during stable isotope analyses. We thank the associate editor, Cinzia Cervato, and two anonymous reviewers for useful comments that improved the manuscript. This research used samples provided by the Integrated Ocean Drilling Program, which is sponsored by the NSF and participating countries under management of the Joint Oceanographic Institutions, Inc.

APPENDIX 1. BENTHIC FORAMINIFERAL STABLE ISOTOPE DATA FOR OCEAN DRILLING PROGRAM SITE 884

| Sample identification | Depth (mbsf) | Depth (cmbsf) | Age (Ma) | $\delta^{18}O$ (‰ VPDB) | $\delta^{13}C$ (‰ VPDB) | Adjusted to *Cibicidoides* spp. $\delta^{18}O$ (‰ VPDB) | Adjusted to *Cibicidoides* spp. $\delta^{13}C$ (‰ VPDB) | Genus and/or species |
|---|---|---|---|---|---|---|---|---|
| *884B 73X-2 103-108 | 673.53 | 673.53 | 32.56 | 1.48 | 0.46 | 1.48 | 0.46 | *Cibicidoides* spp. |
| *884B 73X-3 129-134 | 675.29 | 675.29 | 32.63 | 1.72 | 0.63 | 1.72 | 0.63 | *Cibicidoides* spp. |
| *884B 73X-4 75-80 | 676.25 | 676.25 | 32.68 | 1.53 | 0.38 | 1.53 | 0.38 | *Cibicidoides* spp. |
| *884B 73X-5 33-38 | 677.33 | 677.33 | 32.72 | 1.66 | 0.43 | 1.66 | 0.43 | *Cibicidoides* spp. |
| *884B 74X-1 0-5 | 680.60 | 680.60 | 32.87 | 1.56 | 0.92 | 1.56 | 0.92 | *Cibicidoides* spp. |
| 884B 74-1W 0-2 | 680.60 | 680.60 | 32.87 | 2.03 | 0.84 | 2.03 | 0.84 | *Cibicidoides* spp. |
| 884B 74-1W 70-72 | 681.30 | 681.28 | 32.90 | 0.55 | 0.80 | 0.55 | 0.80 | *Cibicidoides* spp. |
| 884B 74-1W 140-142 | 682.00 | 681.97 | 32.93 | 0.58 | 0.18 | 0.58 | 0.18 | *Cibicidoides* spp. |
| 884B 74-2W 0-2 | 682.10 | 682.07 | 32.93 | 0.42 | –0.10 | 0.14 | 0.62 | *Oridorsalis* spp. |
| 884B 74-2W 70-72 | 682.80 | 682.75 | 32.96 | 0.79 | 0.18 | 0.79 | 0.18 | *Cibicidoides* spp. |
| 884B 74-3W 140-142 | 685.00 | 684.90 | 33.05 | 0.36 | 0.75 | 0.36 | 0.75 | *Cibicidoides* spp. |
| 884B 74-7W 0-2 | 689.60 | 689.40 | 33.24 | 0.86 | 0.58 | 0.86 | 0.58 | *Cibicidoides* spp. |
| *884B 74X-7 10-15 | 689.70 | 689.50 | 33.25 | 1.72 | 0.74 | 1.72 | 0.74 | *Cibicidoides* spp. |
| 884B 74-7W 25-27 | 689.85 | 689.64 | 33.25 | 0.82 | 0.38 | 0.82 | 0.38 | *Cibicidoides* spp. |
| 884B 74-7W 50-52 | 690.10 | 689.89 | 33.26 | 0.77 | 0.28 | 0.77 | 0.28 | *Cibicidoides* spp. |
| 884B 74-CCW 0-2 | 690.13 | 689.92 | 33.26 | 0.80 | 0.25 | 0.80 | 0.25 | *Cibicidoides* spp. |
| 884B 74-CCW 10-12 | 690.23 | 690.01 | 33.27 | 0.85 | –0.02 | 0.85 | –0.02 | *Cibicidoides* spp. |
| 884B 74-CCW 20-22 | 690.33 | 690.11 | 33.27 | 1.04 | 0.14 | 1.04 | 0.14 | *Cibicidoides* spp. |
| 884B 75-2W 0-2 | 691.70 | 691.65 | 33.34 | 0.89 | 0.33 | 0.89 | 0.33 | *Cibicidoides* spp. |
| 884B 75-2W 70-72 | 692.40 | 692.33 | 33.37 | 1.04 | 0.49 | 1.04 | 0.49 | *Cibicidoides* spp. |
| 884B 75-2W 140-142 | 693.10 | 693.01 | 33.40 | 0.75 | 0.12 | 0.95 | 0.46 | *Nuttallides truempyi* |
| 884B 75-3W 0-2 | 693.20 | 693.11 | 33.40 | 0.55 | 0.39 | 0.55 | 0.39 | *Cibicidoides* spp. |
| 884B 75-3W 70-72 | 693.90 | 693.78 | 33.43 | 0.61 | 0.59 | 0.61 | 0.59 | *Cibicidoides* spp. |
| *884B 75X-3 128-133 | 694.48 | 694.35 | 33.45 | 0.91 | 0.84 | 0.91 | 0.84 | *Cibicidoides* spp. |
| 884B 75-3W 140-142 | 694.60 | 694.46 | 33.46 | 0.84 | 0.63 | 0.84 | 0.63 | *Cibicidoides* spp. |
| 884B 75-4W 70-72 | 695.40 | 695.24 | 33.49 | 0.55 | 0.60 | 0.55 | 0.60 | *Cibicidoides* spp. |
| *884B 75X-4 75-80 | 695.45 | 695.29 | 33.49 | 0.31 | 0.51 | 0.31 | 0.51 | *Cibicidoides* spp. |
| *884B 75X-4 75-80 replicate | 695.45 | 695.29 | 33.49 | 0.26 | 0.32 | 0.40 | 0.66 | *Nuttallides truempyi* |

(*continued*)

APPENDIX 1. BENTHIC FORAMINIFERAL STABLE ISOTOPE DATA FOR OCEAN DRILLING PROGRAM SITE 884 (*continued*)

| Sample identification | Depth (mbsf) | Depth (cmbsf) | Age (Ma) | $\delta^{18}O$ (‰ VPDB) | $\delta^{13}C$ (‰ VPDB) | Adjusted to *Cibicidoides* spp. $\delta^{18}O$ (‰ VPDB) | Adjusted to *Cibicidoides* spp. $\delta^{13}C$ (‰ VPDB) | Genus and/or species |
|---|---|---|---|---|---|---|---|---|
| *884B 75X-5 140-145 | 697.60 | 697.37 | 33.58 | 0.40 | 0.31 | 0.56 | 0.65 | *Nuttallides truempyi* |
| 884B 75-5W 140-142 | 697.60 | 697.37 | 33.58 | 0.70 | 0.81 | 0.70 | 0.81 | *Cibicidoides* spp. |
| 884B 75-6W 0-2 | 697.70 | 697.47 | 33.58 | 0.84 | 0.62 | 0.84 | 0.62 | *Cibicidoides* spp. |
| 884B 75-6W 45-47 | 698.15 | 697.90 | 33.60 | 0.39 | 0.08 | 0.39 | 0.08 | *Cibicidoides* spp. |
| *884B 75X-6 84-89 | 698.54 | 698.28 | 33.62 | 0.10 | –0.03 | 0.22 | 0.31 | *Nuttallides truempyi* |
| 884B 75-6W 90-92 | 698.60 | 698.34 | 33.62 | 0.50 | 0.79 | 0.50 | 0.79 | *Cibicidoides* spp. |
| 884B 75-7W 0-2 | 698.70 | 698.43 | 33.63 | 0.47 | 0.77 | 0.47 | 0.77 | *Cibicidoides* spp. |
| *884B 75X-7 12-17 | 698.82 | 698.55 | 33.63 | 0.27 | 0.26 | 0.42 | 0.60 | *Nuttallides truempyi* |
| 884B 75-CCW 0-2 | 699.71 | 699.41 | 33.67 | 0.74 | 0.74 | 0.74 | 0.74 | *Cibicidoides* spp. |
| 884B 75-CCW 15-17 | 699.86 | 699.56 | 33.67 | 0.74 | 0.69 | 0.74 | 0.69 | *Cibicidoides* spp. |
| 884B 75-CCW 30-32 | 700.01 | 699.70 | 33.68 | 0.88 | 0.51 | 0.88 | 0.51 | *Cibicidoides* spp. |
| 884B 76-1W 0-2 | 699.80 | 699.80 | 33.68 | 0.74 | 0.77 | 0.74 | 0.77 | *Cibicidoides* spp. |
| 884B 76-2W 70-72 | 702.00 | 701.94 | 33.77 | 1.48 | 0.28 | 1.48 | 0.28 | *Cibicidoides* spp. |
| 884B 76-2W 140-142 | 702.70 | 702.62 | 33.80 | 1.32 | 0.20 | 1.32 | 0.20 | *Cibicidoides* spp. |
| 884B 76-3W 0-2 | 702.80 | 702.71 | 33.81 | 1.80 | –0.17 | 1.52 | 0.55 | *Oridorsalis* spp. |
| 884B 76-3W 70-72 | 703.50 | 703.39 | 33.84 | 1.37 | 1.04 | 1.37 | 1.04 | *Cibicidoides* spp. |
| 884B 76-5W 70-72 | 706.50 | 706.31 | 33.96 | 1.81 | 0.91 | 1.81 | 0.91 | *Cibicidoides* spp. |
| 884B 77-1W 0-2 | 709.50 | 709.50 | 34.09 | 2.17 | –0.78 | 1.89 | –0.06 | *Oridorsalis* spp. |
| 884B 77-3W 0-2 | 712.50 | 712.35 | 34.22 | 1.11 | 0.61 | 1.11 | 0.61 | *Cibicidoides* spp. |
| 884B 77-3W 70-72 | 713.20 | 713.02 | 34.24 | 0.87 | 0.55 | 0.87 | 0.55 | *Cibicidoides* spp. |
| *884B 77X-3 73-78 | 713.23 | 713.05 | 34.25 | 0.68 | 0.38 | 0.88 | 0.72 | *Nuttallides truempyi* |
| 884B 77-3W 140-142 | 713.90 | 713.69 | 34.27 | 0.81 | 0.11 | 1.02 | 0.45 | *Nuttallides truempyi* |
| 884B 77-4W 0-2 | 714.00 | 713.78 | 34.28 | 1.30 | 0.62 | 1.30 | 0.62 | *Cibicidoides* spp. |
| *884B 77X-5 2-7 | 715.52 | 715.23 | 34.34 | 0.43 | 0.37 | 0.60 | 0.71 | *Nuttallides truempyi* |
| 884B 77-5W 70-72 | 716.20 | 715.87 | 34.36 | 1.74 | –0.29 | 1.46 | 0.43 | *Oridorsalis* spp. |
| 884B 77-5W 140-142 | 716.90 | 716.54 | 34.39 | 0.66 | 0.77 | 0.66 | 0.77 | *Cibicidoides* spp. |
| 884B 77-6W 0-2 | 717.00 | 716.64 | 34.40 | 0.55 | 0.69 | 0.55 | 0.69 | *Cibicidoides* spp. |
| 884B 78-5W 0-2 | 725.10 | 725.10 | 34.76 | 0.74 | 0.00 | 0.94 | 0.34 | *Nuttallides truempyi* |
| 884B 79-3W 70-72 | 732.50 | 732.50 | 35.07 | 0.73 | 0.41 | 0.73 | 0.41 | *Cibicidoides* spp. |
| *884B 79X-3 114-119 | 732.94 | 732.94 | 35.09 | 0.60 | 0.26 | 0.79 | 0.60 | *Nuttallides truempyi* |
| *884B 79X-5 113-118 | 735.93 | 735.93 | 35.20 | 0.19 | 0.56 | 0.33 | 0.90 | *Nuttallides truempyi* |
| 884B 79-5W 140-142 | 736.20 | 736.20 | 35.21 | 0.79 | 0.30 | 0.79 | 0.30 | *Cibicidoides* spp. |
| 884B 79-6W 0-2 | 736.30 | 736.30 | 35.21 | 1.02 | 0.60 | 1.02 | 0.60 | *Cibicidoides* spp. |
| 884B 80-1W 0-2 | 738.40 | 738.40 | 35.28 | 0.96 | 0.36 | 0.96 | 0.36 | *Cibicidoides* spp. |
| *884B 80X-1 53-58 | 738.93 | 738.93 | 35.30 | 0.66 | 0.45 | 0.66 | 0.45 | *Cibicidoides* spp. |
| *884B 80X-4 119-124 | 744.09 | 744.09 | 35.48 | 0.29 | 0.46 | 0.29 | 0.46 | *Cibicidoides* spp. |
| *884B 80X-4 119-124 replicate | 744.09 | 744.09 | 35.48 | 0.13 | 0.19 | 0.26 | 0.53 | *Nuttallides truempyi* |
| 884B 80-4W 130-132 | 744.20 | 744.20 | 35.48 | 0.57 | 0.80 | 0.57 | 0.80 | *Cibicidoides* spp. |
| 884B 80-5W 2-4 | 744.42 | 744.42 | 35.49 | 0.53 | 0.68 | 0.53 | 0.68 | *Cibicidoides* spp. |
| 884B 80-5W 72-74 | 745.12 | 745.12 | 35.52 | 0.21 | 0.57 | 0.21 | 0.57 | *Cibicidoides* spp. |
| *884B 80X-5 75-80 | 745.15 | 745.15 | 35.52 | 0.39 | 0.70 | 0.55 | 1.04 | *Nuttallides truempyi* |
| 884B 80-6W 90-92 | 746.80 | 746.80 | 35.57 | 0.76 | 0.18 | 0.97 | 0.52 | *Nuttallides truempyi* |
| 884B 80-7W 0-2 | 746.90 | 746.90 | 35.58 | 1.00 | 0.58 | 1.00 | 0.58 | *Cibicidoides* spp. |
| 884B 80-7W 25-27 | 747.15 | 747.15 | 35.59 | 0.92 | 0.32 | 0.92 | 0.32 | *Cibicidoides* spp. |
| 884B 80-CCW 0-2 | 747.51 | 747.51 | 35.60 | 0.74 | 0.65 | 0.74 | 0.65 | *Cibicidoides* spp. |
| 884B 81-1W 0-2 | 748.10 | 748.10 | 35.62 | 0.82 | 0.30 | 1.03 | 0.64 | *Nuttallides truempyi* |

(*continued*)

APPENDIX 1. BENTHIC FORAMINIFERAL STABLE ISOTOPE DATA FOR OCEAN DRILLING PROGRAM SITE 884 (*continued*)

| Sample identification | Depth (mbsf) | Depth (cmbsf) | Age (Ma) | $\delta^{18}O$ (‰ VPDB) | $\delta^{13}C$ (‰ VPDB) | Adjusted to *Cibicidoides* spp. $\delta^{18}O$ (‰ VPDB) | Adjusted to *Cibicidoides* spp. $\delta^{13}C$ (‰ VPDB) | Genus and/or species |
|---|---|---|---|---|---|---|---|---|
| *884B 81X-1 138-145 | 749.48 | 749.48 | 35.67 | 0.24 | 0.18 | 0.38 | 0.52 | *Nuttallides truempyi* |
| 884B 81-1W 140-142 | 749.50 | 749.50 | 35.67 | 1.64 | 1.13 | 1.64 | 1.13 | *Cibicidoides* spp. |
| 884B 81-2W 0-2 | 749.60 | 749.60 | 35.67 | –0.18 | 0.57 | –0.18 | 0.57 | *Cibicidoides* spp. |
| 884B 81-2W 70-72 | 750.30 | 750.30 | 35.69 | 0.36 | –0.06 | 0.36 | –0.06 | *Cibicidoides* spp. |
| *884B 81X-2 138-145 | 750.98 | 750.98 | 35.72 | 0.18 | 0.30 | 0.18 | 0.30 | *Cibicidoides* spp. |
| *884B 81X-2 138-145 replicate | 750.98 | 750.98 | 35.72 | 0.02 | –0.16 | 0.13 | 0.18 | Nuttallides truempyi |
| 884B 81-2W 140-142 | 751.00 | 751.00 | 35.72 | 0.40 | 0.25 | 0.40 | 0.25 | *Cibicidoides spp.* |
| 884B 81-3W 0-2 | 751.10 | 751.10 | 35.72 | 0.17 | 0.15 | 0.17 | 0.15 | *Cibicidoides* spp. |
| 884B 81-3W 70-72 | 751.80 | 751.80 | 35.75 | –0.72 | 0.13 | –0.72 | 0.13 | *Cibicidoides* spp. |
| *884B 81X-3 110-115 | 752.20 | 752.20 | 35.76 | 0.27 | 0.40 | 0.42 | 0.74 | *Nuttallides truempyi* |
| *884B 81X-4 50-55 | 753.10 | 753.10 | 35.79 | 0.32 | 0.49 | 0.47 | 0.83 | *Nuttallides truempyi* |
| 884B 81-4W 55-57 | 753.15 | 753.15 | 35.79 | 0.44 | 0.62 | 0.44 | 0.62 | *Cibicidoides* spp. |
| 884B 81-4W 110-112 | 753.70 | 753.70 | 35.81 | –0.14 | 0.83 | –0.14 | 0.83 | *Cibicidoides* spp. |
| 884B 81-5W 0-2 | 753.78 | 753.78 | 35.82 | 0.43 | 0.59 | 0.43 | 0.59 | *Cibicidoides* spp. |
| 884B 81-5W 15-17 | 753.93 | 753.93 | 35.82 | 0.52 | 0.89 | 0.52 | 0.89 | *Cibicidoides* spp. |
| 884B 81-5W 30-32 | 754.08 | 754.08 | 35.83 | 0.70 | 0.78 | 0.70 | 0.78 | *Cibicidoides* spp. |
| 884B 81-CCW 0-2 | 754.14 | 754.14 | 35.83 | 0.29 | 0.73 | 0.29 | 0.73 | *Cibicidoides* spp. |
| 884B 81-CCW 15-17 | 754.29 | 754.29 | 35.83 | 0.66 | 0.92 | 0.66 | 0.92 | *Cibicidoides* spp. |
| 884B 81-CCW 30-32 | 754.44 | 754.44 | 35.84 | 0.48 | 0.24 | 0.48 | 0.24 | *Cibicidoides* spp. |
| 884B 82-1W 0-2 | 757.70 | 757.70 | 35.95 | 0.75 | 0.59 | 0.75 | 0.59 | *Cibicidoides* spp. |
| *884B 82X-1 52-57 | 758.22 | 758.21 | 35.97 | 0.00 | –0.21 | 0.11 | 0.13 | *Nuttallides truempyi* |
| 884B 82-1W 70-72 | 758.40 | 758.39 | 35.97 | –0.17 | 0.35 | –0.17 | 0.35 | *Cibicidoides* spp. |
| 884B 82-2W 16-18 | 759.36 | 759.33 | 36.01 | –0.15 | 0.26 | –0.15 | 0.26 | *Cibicidoides* spp. |
| 884B 82-2W 76-78 | 759.96 | 759.92 | 36.03 | 0.82 | 0.93 | 0.82 | 0.93 | *Cibicidoides* spp. |
| *884B 82-2W 105-110 | 760.25 | 760.21 | 36.04 | 0.11 | 0.03 | 0.11 | 0.03 | *Cibicidoides* spp. |
| 884B 82-2W 136-138 | 760.56 | 760.51 | 36.05 | 0.23 | 0.21 | 0.23 | 0.21 | *Cibicidoides* spp. |
| 884B 82-3W 3-5 | 760.73 | 760.68 | 36.05 | 0.37 | –0.05 | 0.37 | –0.05 | *Cibicidoides* spp. |
| 884B 82-3W 53-55 | 761.23 | 761.17 | 36.07 | 0.40 | 0.02 | 0.40 | 0.02 | *Cibicidoides* spp. |
| *884B 82X-3 107-112 | 761.77 | 761.70 | 36.09 | 0.13 | –0.17 | 0.26 | 0.17 | *Nuttallides truempyi* |
| *884B 82X-3 107-112 replicate | 761.77 | 761.70 | 36.09 | 0.19 | –0.10 | 0.33 | 0.24 | *Nuttallides truempyi* |
| 884B 82-4W 2-4 | 762.22 | 762.15 | 36.10 | 0.30 | –0.08 | 0.30 | –0.08 | *Cibicidoides* spp. |
| *884B 82X-4 79-84 | 762.99 | 762.90 | 36.46 | 0.07 | 0.07 | 0.19 | 0.41 | *Nuttallides truempyi* |
| 884B 82-5W 1-3 | 763.71 | 763.61 | 36.86 | –0.16 | 0.45 | –0.16 | 0.45 | *Cibicidoides* spp. |
| 884B 82-5W 51-53 | 764.21 | 764.10 | 37.15 | –0.17 | 0.30 | –0.17 | 0.30 | *Cibicidoides* spp. |
| 884B 82-6W 50-52 | 765.70 | 765.57 | 37.99 | 0.15 | 0.15 | 0.15 | 0.15 | *Cibicidoides* spp. |
| 884B 82-6W 100-102 | 766.20 | 766.06 | 38.27 | 0.25 | 0.21 | 0.25 | 0.21 | *Cibicidoides* spp. |
| *884B 82X-6 134-139 | 766.54 | 766.40 | 38.47 | –0.38 | 0.42 | –0.31 | 0.76 | *Nuttallides truempyi* |
| 884B 82-7W 0-2 | 766.70 | 766.55 | 38.55 | 0.26 | 0.75 | 0.26 | 0.75 | *Cibicidoides* spp. |
| 884B 82-7W 20-22 | 766.90 | 766.75 | 38.67 | 0.10 | 0.16 | 0.10 | 0.16 | *Cibicidoides* spp. |
| 884B 82-7W 40-42 | 767.10 | 766.95 | 38.78 | 0.13 | 0.22 | 0.13 | 0.22 | *Cibicidoides* spp. |
| 884B 82-CCW 0-2 | 767.14 | 766.99 | 38.81 | –0.40 | 0.45 | –0.40 | 0.45 | *Cibicidoides* spp. |
| 884B 82-CCW 15-17 | 767.29 | 767.14 | 38.89 | 0.42 | 0.33 | 0.42 | 0.33 | *Cibicidoides* spp. |
| 884B 82-CCW 30-32 | 767.44 | 767.28 | 38.97 | –0.03 | 0.36 | –0.03 | 0.36 | *Cibicidoides* spp. |
| 884B 83-1W 3-5 | 767.43 | 767.43 | 39.06 | –0.12 | 0.19 | –0.12 | 0.19 | *Cibicidoides* spp. |
| 884B 83-1W 53-55 | 767.93 | 767.92 | 39.34 | 0.01 | 0.11 | 0.01 | 0.11 | *Cibicidoides* spp. |
| *884B 83X-1 72-77 | 768.12 | 768.11 | 39.45 | –0.12 | 0.08 | –0.02 | 0.42 | *Nuttallides truempyi* |

(*continued*)

APPENDIX 1. BENTHIC FORAMINIFERAL STABLE ISOTOPE DATA FOR OCEAN DRILLING PROGRAM SITE 884 (*continued*)

| Sample identification | Depth (mbsf) | Depth (cmbsf) | Age (Ma) | $\delta^{18}O$ (‰ VPDB) | $\delta^{13}C$ (‰ VPDB) | Adjusted to *Cibicidoides* spp. $\delta^{18}O$ (‰ VPDB) | Adjusted to *Cibicidoides* spp. $\delta^{13}C$ (‰ VPDB) | Genus and/or species |
|---|---|---|---|---|---|---|---|---|
| 884B 83-1W 103-105 | 768.43 | 768.42 | 39.63 | 0.46 | 0.42 | 0.46 | 0.42 | *Cibicidoides* spp. |
| 884B 83-2W 6-8 | 768.96 | 768.94 | 39.90 | –0.05 | 0.25 | –0.05 | 0.25 | *Cibicidoides* spp. |
| *884B 83X-2 26-31 | 769.16 | 769.14 | 40.02 | –0.05 | –0.08 | 0.06 | 0.26 | *Nuttallides truempyi* |
| 884B 83-2W 56-58 | 769.46 | 769.44 | 40.19 | 0.15 | 0.18 | 0.15 | 0.18 | *Cibicidoides* spp. |
| 884B 83-2W 106-108 | 769.96 | 769.93 | 40.47 | 0.32 | 0.62 | 0.32 | 0.62 | *Cibicidoides* spp. |
| 884B 83-3W 7-9 | 770.47 | 770.44 | 40.76 | 0.42 | –0.09 | 0.42 | –0.09 | *Cibicidoides* spp. |
| 884B 83-3W 57-59 | 770.97 | 770.93 | 41.04 | 0.29 | 0.14 | 0.29 | 0.14 | *Cibicidoides* spp. |
| 884B 83-3W 107-109 | 771.47 | 771.42 | 41.33 | 0.21 | 0.30 | 0.21 | 0.30 | *Cibicidoides* spp. |
| 884B 83-4W 1-3 | 771.91 | 771.86 | 41.58 | –0.02 | 0.30 | –0.02 | 0.30 | *Cibicidoides* spp. |
| 884B 83-4W 51-53 | 772.41 | 772.35 | 41.86 | 0.22 | 0.11 | 0.22 | 0.11 | *Cibicidoides* spp. |
| 884B 83-4W 101-103 | 772.91 | 772.85 | 42.15 | 0.56 | 0.09 | 0.56 | 0.09 | *Cibicidoides* spp. |
| 884B 83-5W 2-4 | 773.42 | 773.35 | 42.44 | 0.78 | –0.02 | 0.78 | –0.02 | *Cibicidoides* spp. |
| 884B 83-5W 52-54 | 773.92 | 773.85 | 42.72 | 0.61 | 0.18 | 0.61 | 0.18 | *Cibicidoides* spp. |
| 884B 83-5W 102-104 | 774.42 | 774.34 | 43.01 | 0.39 | 0.03 | 0.39 | 0.03 | *Cibicidoides* spp. |
| 884B 83-6W 2-4 | 774.92 | 774.84 | 43.29 | 0.25 | 0.01 | 0.25 | 0.01 | *Cibicidoides* spp. |
| 884B 83-6W 42-44 | 775.32 | 775.23 | 43.52 | 0.49 | –0.03 | 0.49 | –0.03 | *Cibicidoides* spp. |
| 884B 83-6W 82-84 | 775.72 | 775.63 | 43.75 | 0.65 | –0.02 | 0.65 | –0.02 | *Cibicidoides* spp. |
| 884B 83-7W 1-3 | 775.76 | 775.67 | 43.77 | 0.42 | 0.06 | 0.42 | 0.06 | *Cibicidoides* spp. |
| 884B 83-7W 41-43 | 776.16 | 776.06 | 43.99 | 0.21 | 0.12 | 0.21 | 0.12 | *Cibicidoides* spp. |
| 884B 83-7W 81-83 | 776.56 | 776.46 | 44.22 | 0.30 | 0.10 | 0.30 | 0.10 | *Cibicidoides* spp. |
| 884B 83-CCW 0-2 | 776.64 | 776.54 | 44.27 | 0.21 | 0.03 | 0.21 | 0.03 | *Cibicidoides* spp. |
| 884B 83-CCW 20-22 | 776.84 | 776.73 | 44.38 | 0.19 | 0.02 | 0.19 | 0.02 | *Cibicidoides* spp. |
| 884B 83-CCW 40-42 | 777.04 | 776.93 | 44.49 | 0.61 | 0.02 | 0.61 | 0.02 | *Cibicidoides* spp. |
| 884B 84-1W 4-6 | 777.04 | 777.04 | 44.56 | 0.58 | 0.89 | 0.58 | 0.89 | *Cibicidoides* spp. |
| 884B 84-2W 3-5 | 778.53 | 778.50 | 45.40 | 0.69 | –0.07 | 0.89 | 0.27 | *Nuttallides truempyi* |
| 884B 84-2W 53-55 | 779.03 | 778.99 | 45.68 | 0.14 | 0.18 | 0.14 | 0.18 | *Cibicidoides* spp. |
| 884B 84-2W 103-105 | 779.53 | 779.48 | 45.96 | –0.01 | –0.06 | –0.01 | –0.06 | *Cibicidoides* spp. |
| 884B 84-3W 2-4 | 780.02 | 779.96 | 46.24 | 0.28 | 0.08 | 0.28 | 0.08 | *Cibicidoides* spp. |
| 884B 84-3W 52-54 | 780.52 | 780.45 | 46.52 | 0.25 | –0.03 | 0.25 | –0.03 | *Cibicidoides* spp. |
| *884B 84X-5 100-105 | 784.00 | 783.85 | 48.47 | –0.33 | 0.13 | –0.26 | 0.47 | *Nuttallides truempyi* |
| 884B 84-5W 102-104 | 784.02 | 783.87 | 48.49 | –0.30 | 0.18 | –0.30 | 0.18 | *Cibicidoides* spp. |
| 884B 84-6W 0-2 | 784.50 | 784.34 | 48.76 | 0.08 | 0.25 | 0.08 | 0.25 | *Cibicidoides* spp. |
| 884B 84-6W 100-102 | 785.50 | 785.32 | 49.32 | 0.25 | 0.27 | 0.25 | 0.27 | *Cibicidoides* spp. |

*Note:* The *Nuttallides truempyi* and *Oridorsalis* spp. data are corrected to *Cibicidoides* spp. using the calibration of Katz et al. (2003). VPDB—Vienna Pee Dee Belemnite; mbsf—meters below seafloor; cmbsf—compacted mbsf.

*Site 884 data of Pak and Miller (1995).

**REFERENCES CITED**


Aubry, M.-P., and Bord, D., 2009, Reshuffling the cards in the photic zone at the Eocene/Oligocene boundary, *in* Koeberl, C., and Montanari, A., eds., The late Eocene Earth—Hothouse, icehouse and impacts: Geological Society of America Special Paper 452, p. 279–301, doi:10.1130/2009.2452(18).

Barron, J.A., Larsen, B., and Baldauf, J.G., 1991, Evidence for late Eocene to early Oligocene Antarctic glaciation and observations of late Neogene glacial history of Antarctica: Results from Leg 119, *in* Barron, J., et al., Proceedings of the Ocean Drilling Program, Scientific results, Volume 119: College Station, Texas, Ocean Drilling Program, p. 869–891, doi:10.2973/odp.proc.sr.119.194.1991.

Barron, J.A., et al., 1995, Biostratigraphic and magnetostratigraphic summary, *in* Rea, D.K., et al., Proceedings of the Ocean Drilling Program, Scientific results, Volume 145: College Station, Texas, Ocean Drilling Program, p. 559–575, doi:10.2973/odp.proc.sr.145.145.1995.

Basov, I.A., 1995, Paleogene planktonic foraminifera biostratigraphy of Sites 883 and 884, Detroit Seamount (Subartic Pacific), *in* Rea, D.K., et al., Proceedings of the Ocean Drilling Program, Scientific results, Volume 145: College Station, Texas, Ocean Drilling Program, p. 157–170, doi:10.2973/odp.proc.sr.145.112.1995.

Beaufort, L., and Ólafsson, G., 1995, Data report: Upper Cretaceous and Paleogene calcareous nannofossils from the North Pacific, *in* Rea, D.K., et al., Proceedings of the Ocean Drilling

Program, Scientific results, Volume 145: College Station, Texas, Ocean Drilling Program, p. 633–638, doi:10.2973/odp.proc.sr.145.103.1995.

Berggren, W.A., Kent, D.V., Swisher, C.C., and Aubry, M.-P., 1995, A revised Cenozoic geochronology and chronostratigraphy, *in* Berggren, W.A., et al., eds., Geochronology, time scales and global stratigraphic correlations: A unified temporal framework for an historical geology: SEPM (Society for Sedimentary Geology) Special Publication 54, p. 129–212, doi:10.2110/pec.95.04.0129.

Bijl, P.K., et al., 2013, Eocene cooling linked to early flow across the Tasmanian Gateway: National Academy of Sciences Proceedings, v. 110, p. 9645–9650, doi:10.1073/pnas.1220872110.

Billups, K., Channell, J.E.T., and Zachos, J., 2002, Late Oligocene to early Miocene geochronology and paleoceanography from the subantarctic South Atlantic: Paleoceanography, v. 17, p. 1004, doi:10.1029/2000PA000568.

Bohaty, S.M., and Zachos, J.C., 2003, Significant Southern Ocean warming event in the late middle Eocene: Geology, v. 31, p. 1017–1020, doi:10.1130/G19800.1.

Bohaty, S.M., Zachos, J.C., Florindo, F., and Delaney, M.L., 2009, Coupled greenhouse warming and deep-sea acidification in the middle Eocene: Paleoceanography, v. 24, PA2207, doi:10.1029/2008PA001676.

Bohaty, S.M., Zachos, J.C., and Delaney, M.L., 2012, Foraminiferal Mg/Ca evidence for Southern Ocean cooling across the Eocene-Oligocene transition: Earth and Planetary Science Letters, v. 317, p. 251–261, doi:10.1016/j.epsl.2011.11.037.

Borrelli, C., Cramer, B.S., and Katz, M.E., 2014, Bipolar Atlantic deepwater circulation in the middle-late Eocene: Effects of Southern Ocean opening: Paleoceanography, v. 29, p. 308–327, doi:10.1002/2012PA002444.

Bralower, T.J., 2005, Data report: Paleocene–early Oligocene calcareous nannofossil biostratigraphy, ODP Leg 198 Sites 1209, 1210, and 1211 (Shatsky Rise, Pacific Ocean), *in* Bralower, T.J., et al., Proceedings of the Ocean Drilling Program, Scientific results, Volume 198: College Station, Texas, Ocean Drilling Program, p. 1–15, doi:10.2973/odp.proc.sr.198.115.2005.

Bralower, T.J., Zachos, J.C., Thomas, E., Parrow, M., Paull, C.K., Kelly, D.C., Premoli Silva, I., Sliter, W.V., and Lohmann, K.C., 1995, Late Paleocene to Eocene paleoceanography of the equatorial Pacific Ocean: Stable isotopes recorded at Ocean Drilling Program Site 865, Allison Guyot: Paleoceanography, v. 10, p. 841–865, doi:10.1029/95PA01143.

Broecker, W.S., 1991, The great ocean conveyor: Oceanography, v. 4, p. 79–89, doi:10.5670/oceanog.1991.07.

Browning, J.V., Miller, K.G., and Pak, D.K., 1996, Global implication of the lower to middle Eocene sequence boundaries on the New Jersey coastal plain: The icehouse cometh: Geology, v. 24, p. 639–642, doi:10.1130/0091-7613(1996)024<0639:GIOLTM>2.3.CO;2.

Cande, S.C., and Kent, K.D., 1995, Revised calibration of the geomagnetic polarity timescale for the Late Cretaceous and Cenozoic: Journal of Geophysical Research, v. 110, no. B4, p. 6093–6095, doi:10.1029/95PA01143.

Carter, L., Carter, R.M., and McCave, I.N., 2004, Evolution of the sedimentary system beneath the deep Pacific inflow off eastern New Zealand: Marine Geology, v. 205, p. 9–27, doi:10.1016/S0025-3227(04)00016-7.

Channell, J.E.T., Galeotti, S., Martin, E.E., Billups, K., Scher, H.D., and Stoner, J.S., 2003, Eocene to Miocene magnetostratigraphy, biostratigraphy, and chemostratigraphy at ODP Site 1090 (sub-Antarctic South Atlantic): Geological Society of America Bulletin, v. 115, p. 607–623, doi:10.1130/0016-7606(2003)115<0607:ETMMBA>2.0.CO;2.

Cox, M.D., 1989, An idealized model of the world ocean. Part I: The global-scale water masses: Journal of Physical Oceanography, v. 19, p. 1730–1752, doi:10.1175/1520-0485(1989)019<1730:AIMOTW>2.0.CO;2.

Coxall, H.K., and Wilson, P.A., 2011, Early Oligocene glaciation and productivity in the eastern equatorial Pacific: Insights into the carbon cycling: Paleoceanography, v. 26, PA2221, doi:10.1029/2010PA002021.

Coxall, H.K., Wilson, P.A., Pälike, H., Lear, C.H., and Backman, J., 2005, Rapid stepwise onset of Antarctic glaciation and deeper calcite compensation in the Pacific Ocean: Nature, v. 433, no. 7021, p. 53–57, doi:10.1038/nature03135.

Cramer, B.S., Toggweiler, J.R., Wright, J.D., Katz, M.E., and Miller, K.G., 2009, Ocean overturning since the Late Cretaceous: Inferences from a new benthic foraminiferal isotope compilation: Paleoceanography, v. 24, PA4216, doi:10.1029/2008PA001683.

Cramer, B.S., Miller, K.G., Barrett, P.J., and Wright, J.D., 2011, Late Cretaceous–Neogene trends in deep ocean temperature and continental ice volume: Reconciling records of benthic foraminiferal geochemistry ($\delta^{18}O$ and Mg/Ca) with sea level history: Journal of Geophysical Research, v. 116, C12023, doi:10.1029/2011JC007255.

Curry, W.B., and Lohmann, G.P., 1982, Carbon isotopic changes in benthic foraminifera from the western South Atlantic: Reconstruction of glacial abyssal circulation patterns: Quaternary Research, v. 18, p. 218–235, doi:10.1016/0033-5894(82)90071-0.

Dawber, C.F., and Tripati, A.K., 2011, Constraints on glaciation in the middle Eocene (46–37 Ma) from Ocean Drilling Program (ODP) Site 1209 in the tropical Pacific Ocean: Paleoceanography, v. 26, PA2208, doi:10.1029/2010PA002037.

de Boer, A.M., Toggweiler, J.R., and Sigman, D.M., 2008, Atlantic dominance of the meridional overturning circulation: Journal of Physical Oceanography, v. 38, p. 435–450, doi:10.1175/2007JPO3731.1.

DeConto, R.M., and Pollard, D., 2003, Rapid Cenozoic glaciation of Antarctica induced by declining atmospheric $CO_2$: Nature, v. 421, no. 6920, p. 245–249, doi:10.1038/nature01290.

DeConto, R.M., Pollard, D., Wilson, P.A., Pälike, H., Lear, C.H., and Pagani, M., 2008, Thresholds for Cenozoic bipolar glaciation: Nature, v. 455, no. 7213, p. 652–656, doi:10.1038/nature07337.

Dickson, R.R., and Brown, J., 1994, The production of North Atlantic Deep Water: Sources, rates, and pathways: Journal of Geophysical Research, v. 99, no. C6, p. 12,319–12,341, doi:10.1029/94JC00530.

Diester-Haass, L., and Zahn, R., 1996, Eocene-Oligocene transition in the Southern Ocean: History of water mass circulation and biological productivity: Geology, v. 24, p. 163–166, doi:10.1130/0091-7613(1996)024<0163:EOTITS>2.3.CO;2.

Dutton, A., Lohmann, K.C., and Leckie, R.M., 2005, Data report: Stable isotope and Mg/Ca of Paleocene and Eocene foraminifers, ODP Site 1209, Shatsky Rise, *in* Bralower, T.J., et al., Proceedings of the Ocean Drilling Program, Scientific results, Volume 198: College Station, Texas, Ocean Drilling Program, p. 1–19, doi:10.2973/odp.proc.sr.198.119.2005.

Ehrmann, W.U., and Mackensen, A., 1992, Sedimentological evidence for the formation of an East Antarctic ice-sheet in Eocene/Oligocene time: Palaeogeography, Palaeoclimatology, Palaeoecology, v. 93, p. 85–112, doi:10.1016/0031-0182(92)90185-8.

Elderfield, H., Yu, J., Anand, P., Kiefer, T., and Nyland, B., 2006, Calibrations for benthic foraminiferal Mg/Ca paleothermometry and the carbonate ion hypothesis: Earth and Planetary Science Letters, v. 250, p. 633–649, doi:10.1016/j. epsl.2006.07.041.

Exon, N., Kennett, J., and Malone, M., 2004, Leg 189 synthesis: Cretaceous–Holocene history of the Tasmanian gateway, *in* Exon, N., et al., Proceedings of the Ocean Drilling Program, Scientific results, Volume 189: College Station, Texas, Ocean Drilling Program, p. 1–37, doi:10.2973/odp.proc.sr.189.101.2004.

Florindo, F., and Roberts, A.P., 2005, Eocene-Oligocene magnetobiochronology of ODP Sites 689 and 690, Maud Rise, Weddell Sea, Antarctica: Geological Society of America Bulletin, v. 117, p. 46–66, doi:10.1130/B25541.1.

Gordon, A.L., 1991, The role of thermohaline circulation in global climate change: Palisades, New York, Lamont-Doherty Geological Observatory Biennial Report, p. 44–51.

Hague, A.M., Thomas, D.J., Huber, M., Korty, R., Woodard, S.C., and Jones, L.B., 2012, Convection of North Pacific deep water during the early Cenozoic: Geology, v. 40, p. 527–530, doi:10.1130/G32886.1.

Hamilton, T.S., 1995, Seismic stratigraphy of Cenozoic sediments from North Pacific Seamount platform and deep-see sites, Leg 145, *in* Rea, D.K., et al., Proceedings of the Ocean Drilling Program, Scientific results, Volume 145: College Station, Texas, Ocean Drilling Program, p. 437–453, doi:10.2973/odp.proc.sr.145.136.1995.

Haug, G.H., and Tiedmann, R., 1998, Effect of the formation of the Isthmus of Panama on Atlantic Ocean thermohaline circulation: Nature, v. 393, no. 6686, p. 673–676, doi:10.1038/31447.

Hodell, D.A., and Venz-Curtis, K.A., 2006, Late Neogene history of deepwater ventilation in the Southern Ocean: Geochemistry, Geophysics, Geosystems, v. 7, Q09001, doi:10.1029/2005GC001211.

Hönisch, B., Bijma, J., Russell, A.D., Spero, H.J., Palmer, M.R., Zeebe, R.E., and Eisenhauer, A., 2003, The influence of symbiont photosynthesis on the boron isotopic composition of foraminifera shells: Marine Micropaleontology, v. 49, p. 87–96, doi:10.1016/S0377-8398(03)00030-6.

Hopkins, D.M., 1959, Cenozoic history of the Bering Land Bridge: Science, v. 129, no. 3362, p. 1519–1528, doi:10.1126/science.129.3362.1519.

Katz, M.E., Katz, D.R., Wright, J.D., Miller, K.G., Pak, D.K., Shackleton, N.J., and Thomas, E., 2003, Early Cenozoic benthic foraminiferal isotopes: Species reliability and interspecies correction factors: Paleoceanography, v. 18, 1024, doi:10.1029/2002PA000798.

Katz, M.E., Miller, K.G., Wright, J.D., Wade, B.S., Browning, J.V., Cramer, B.S., and Rosenthal, Y., 2008, Stepwise transition from the Eocene greenhouse to the Oligocene icehouse: Nature Geoscience, v. 1, p. 329–334, doi:10.1038/ngeo179.

Katz, M.E., Cramer, B.S., Toggweiler, J.R., Esmay, G., Chengjie, L., Miller, K.G., Rosenthal, Y., Wade, B.S., and Wright, J.D., 2011, Impact of Antarctic Circumpolar Current development on late Paleogene ocean structure: Science, v. 332, no. 6033, p. 1076–1079, doi:10.1126/science.1202122.

Kominz, M.A., and Pekar, S., 2001, Oligocene eustasy from two-dimensional sequence stratigraphic backstripping: Geological Society of America Bulletin, v. 113, p. 291–304, doi:10.1130/0016-7606(2001)113<0291:OEFTDS>2.0.CO;2.

Kroopnick, P.M., 1985, The distribution of $^{13}C$ of $\Sigma CO2$ in the world oceans: Deep-Sea Research, v. 32, p. 57–84, doi:10.1016/0198-0149(85)90017-2.

Kuhlbrodt, T., Griesel, A., Montoya, M., Levermann, A., Hoffman, M., and Rahmstorf, S., 2007, On the driving processes of the Atlantic meridional overturning circulation: Reviews of Geophysics, v. 45, RG2001, doi:10.1029/2004RG000166.

Lear, C.H., Elderfield, H., and Wilson, P.A., 2000, Cenozoic deep-sea temperatures and global ice volumes from Mg/Ca in benthic foraminiferal calcite: Science, v. 287, no. 5451, p. 269–272, doi:10.1126/science.287.5451.269.

Lear, C.H., Rosenthal, Y., Coxall, H.K., and Wilson, P.A., 2004, Late Eocene to early Miocene ice sheet dynamics and the global carbon cycle: Paleoceanography, v. 19, doi:10.1029/2004PA001039.

Lear, C.H., Bailey, T.R., Pearson, P.H., Coxall, H.K., and Rosenthal, Y., 2008, Cooling and ice-sheet growth across the Eocene-Oligocene transition: Geology, v. 36, p. 251–254, doi:10.1130/G24584A.1.

Liu, Z., Pagani, M., Zanniker, D., DeConto, R., Huber, M., Brinkhuis, H., Shah, S.R., Leckie, R.M., and Pearson, A., 2009, Global cooling during the Eocene-Oligocene climate transition: Science, v. 323, no. 5918, p. 1187–1190, doi:10.1126/science.1166368.

Livermore, R., Hillenbrand, C.-D., Meredith, M., and Eagles, G., 2007, Drake Passage and Cenozoic climate: An open and shut case?: Geochemistry, Geophysics, Geosystems, v. 8, Q01005, doi:10.1029/2005GC001224.

Lunt, D.J., Valdes, P.J., Haywood, A., and Rutt, I.C., 2008, Closure of the Panama Seaway during the Pliocene: Implications for climate and Northern Hemisphere glaciation: Climate Dynamics, v. 30, p. 1–18, doi:10.1007/s00382-007-0265-6.

Lyle, M., Barron, J., Bralower, T.J., Huber, M., Olivarez Lyle, A., Ravelo, A.C., Rea, D.K., and Wilson, P.A., 2008, Pacific Ocean and Cenozoic evolution of climate: Reviews of Geophysics, v. 46, RG2002, doi:10.1029/2005RG000190.

Lynch-Stieglitz, J., Curry, W.B., and Slowey, N., 1999, A geostrophic transport estimate for the Florida Current from the oxygen isotope composition of benthic foraminifera: Paleoceanography, v. 14, p. 360–373, doi:10.1029/1999PA900001.

Mammerickx, J., 1985, A deep-sea thermohaline flow path in the Northwest Pacific: Marine Geology, v. 65, p. 1–19, doi:10.1016/0025-3227(85)90043-X.

Martin, E.E., and Haley, B.A., 2000, Fossil fish teeth as proxies for seawater Sr and Nd isotopes: Geochimica et Cosmochimica Acta, v. 64, p. 835–847, doi:10.1016/S0016-7037(99)00376-2.

Menviel, L., Timmermann, A., Timm, O.E., Mouchet, A., Abe-Ouchi, A., Chikamoto, M.O., Harada, N., Ohgaito, R., and Okazaki, Y., 2012, Removing the North Pacific halocline: Effects on global climate, ocean circulation and the carbon cycle: Deep-sea Research, v. 61–64, p. 106–113, doi:10.1016/j.dsr2.2011.03.005.

Miller, K.G., 1992, Middle Eocene to Oligocene stable isotopes, climate, and deep-water history: The terminal Eocene event?, *in* Prothero, D.R., and Berggren, W.A., eds., Eocene–Oligocene climatic and biotic evolution: Princeton, New Jersey, Princeton University Press, p. 160–177.

Miller, K.G., and Fairbanks, R.G., 1985, Oligocene to Miocene global carbon isotope cycles and abyssal circulation changes, *in* Sundquist, E.T., and Broecker, W.S., eds., The carbon cycle and atmospheric $CO_2$: Natural variation Archean to Present: American Geophysical Union Geophysical Monograph 32, p. 469–486, doi:10.1029/GM032p0469.

Miller, K.G., and Katz, M.E., 1987, Eocene benthic foraminiferal biofacies of the New Jersey transect, *in* Poag, C.W., et al., eds., Initial reports of the Deep Sea Drilling Project, Volume 95: Washington, D.C., U.S. Government Printing Office, p. 267–297, doi:10.2973/dsdp.proc.95.107.1987.

Miller, K.G., Katz, M.E., and Berggren, W.A., 1992, Cenozoic deep-sea benthic foraminifera: A tale of three turnovers, *in* Studies in benthic foraminifera, BENTHOS '90: Sendai, Japan, Tokai University Press, p. 67–75.

Miller, K.G., Kominz, M.A., Browing, J.V., Wright, J.D., Mountain, G.S., Katz, M.E., Sugarman, P.J., Cramer, B.S., Christie-Blick, N., and Pekar, S.F., 2005, The Phanerozoic record of global sea-level change: Science, v. 310, no. 5752, p. 1293–1298, doi:10.1126/science.1116412.

Miller, K.G., Wright, J.D., Katz, M.E., Browning, J.V., Cramer, B.S., Wade, B.S., and Mizintseva, S.F., 2008a, A view of Antarctic ice-sheet evolution from sea-level and deep-sea isotope changes during the Late Cretaceous–Cenozoic, *in* Cooper, A., et al., eds., Antarctica: A Keystone in a Changing World. Proceedings of the 10th International Symposium on Antarctic Earth Sciences: U.S. Geological Survey Open-File Report 2007-1047, p. 55–70, doi:10.3133/of2007-1047.kp06.

Miller, K.G., Browning, J.V., Aubry, M.-P., Wade, B.S., Katz, M.E., Kulpecz, A.A., and Wright, J.D., 2008b, Eocene-Oligocene global climate and sea-level changes: St. Stephens Quarry, Alabama: Geological Society of America Bulletin, v. 120, p. 34–53, doi:10.1130/B26105.1.

Miller, K.G., Wright, J.D., Katz, M.E., Wade, B.S., Browning, J.V., Cramer, B.S., and Rosenthal, Y., 2009, Climate threshold at the Eocene-Oligocene transition: Antarctic ice sheet influence on ocean circulation, *in* Koeberl, C., and Montanari, A., eds., The Late Eocene Earth—Hothouse, icehouse, and impacts: Geological Society of America Special Paper 452, p. 1–10, doi:10.1130/2009.2452(11).

Motoi, T., Chan, W.-L., Minobe, S., and Sumata, H., 2005, North Pacific halocline and cold climate induced by Panamanian Gateway closure in a coupled ocean-atmosphere GCM: Geophysical Research Letters, v. 32, L10618, doi:10.1029/2005GL022844.

Nong, G.T., Najjar, R.G., Seidov, D., and Peterson, W.H., 2000, Simulation of ocean temperature change due to the opening of Drake Passage: Geophysical Research Letters, v. 27, p. 2689–2692, doi:10.1029/1999GL011072.

Ogg, J.G., and Bardot, L., 2001, Aptian through Eocene magnetostratigraphic correlation of the Blake Nose Transect (Leg 171B), Florida continental margin, *in* Kroon, D., et al., Proceedings of the Ocean Drilling Program, Scientific results, Volume 171B: College Station, Texas, Ocean Drilling Program, p. 1–58, doi:10.2973/odp.proc.sr.171b.104.2001.

Oppo, D.W., and Fairbanks, R.G., 1987, Variability in the deep and intermediate water circulation of the Atlantic Ocean during the past 25,000 years: Northern Hemisphere modulation of the Southern Ocean: Earth and Planetary Science Letters, v. 86, p. 1–15, doi:10.1016/0012-821X(87)90183-X.

Owens, W.B., and Warren, B.A., 2001, Deep circulation in the northwestern corner of the Pacific Ocean: Deep-Sea Research, v. 48, p. 959–993, doi:10.1016/S0967-0637(00)00076-5.

Pagani, M., Huber, M., Liu, Z., Bohaty, S.M., Heinderiks, J., Sijp, W., Krishnan, S., and DeConto, R.M., 2011, The role of carbon dioxide during the onset of Antarctic glaciation: Science, v. 334, no. 6060, p. 1261–1264, doi:10.1126/science.1203909.

Pak, D.K., and Miller, K.G., 1995, Isotopic and faunal record of Paleogene deep-water transitions in the North Pacific, *in* Rea, D.K., et al., Proceedings of the Ocean Drilling Program, Scientific results, Volume 145: College Station, Texas, Ocean Drilling Program, p. 265–281, doi:10.2973/odp.proc.sr.145.121.1995.

Pälike, H., Moore, T., Backman, J., Raffi, I., Lanci, L., Parés, J.M., and Janecek, T., 2005, Integrated stratigraphic correlation and improved composite depth scales for ODP Sites 1218 and 1219, *in* Wilson, P.A., et al., Proceedings of the Ocean Drilling Program, Scientific results, Volume 199: College Station, Texas, Ocean Drilling Program, p. 1–42, doi:10.2973/odp.proc.sr.199.213.2005.

Pearson, P.N., Foster, G.L., and Wade, B.S., 2009, Atmospheric carbon dioxide through the Eocene-Oligocene transition: Nature, v. 461, no. 7267, p. 1110–1113, doi:10.1038/nature08447.

Poore, H.R., Samworth, R., White, N.J., Jones, S.M., and McCave, I.N., 2006, Neogene overflow of Northern Component Water at the Greenland-Scotland Ridge: Geochemistry, Geophysics, Geosystems, v. 7, Q06010, doi:10.1029/2005GC001085.

Pusz, A.E., Thunell, R.C., and Miller, K.G., 2011, Deep water temperature, carbonate ion, and ice volume changes, across the Eocene-Oligocene transition: Paleoceanography, v. 26, PA2205, doi:10.1029/2010PA001950.

Rea, D.K., et al., 1993, Proceedings of the Ocean Drilling Program, Initial reports, Volume 145: College Station, Texas, Ocean Drilling Program, doi:10.2973/odp.proc.ir.145.1993.

Rea, D.K., Basov, I.A., Krissek, L.A., and the Leg 145 Scientific Party, 1995, Proceedings of the Ocean Drilling Program, Scientific results, Volume 145: College Station, Texas, Ocean Drilling Program, p. 577–596, doi:10.2973/odp.proc.sr.145.1995.

Reid, J.L., and Lynn, R.J., 1971, On the influence of the Norwegian-Greenland and Weddell seas upon the bottom waters of the Indian and Pacific oceans: Deep-Sea Research, v. 18, p. 1063–1088, doi:10.1016/0011-7471(71)90094-5.

Rosenthal, Y., et al., 2004, Interlaboratory comparison study of Mg/Ca and Sr/Ca measurements in planktonic foraminifera for paleoceanographic research: Geochemistry, Geophysics, Geosystems, v. 5, Q04D09, doi:10.1029/2003GC000650.

Rosenthal, Y., Lear, C.H., Oppo, D.W., and Linsley, B., 2006, Temperature and carbonate ion effects on Mg/Ca and Sr/Ca ratios in benthic foraminifera: Aragonitic species *Hoeglundina elegans*: Paleoceanography, v. 21, PA1007, doi:10.1029/2005PA001158.

Saenko, O.A., Schmittner, A., and Weaver, A.J., 2004, The Atlantic-Pacific seesaw: Journal of Climate, v. 17, p. 2033–2038, doi:10.1175/1520-0442(2004)017<2033:TAS>2.0.CO;2.

Scher, H.D., and Martin, E.E., 2006, Timing and climatic consequences of the opening of Drake Passage: Science, v. 312, no. 5772, p. 428–430, doi:10.1126/science.1120044.

Scher, H.D., and Martin, E.E., 2008, Oligocene deep water export from the North Atlantic and the development of the Antarctic Circumpolar Current examined with neodymium isotopes: Paleoceanography, v. 23, PA1205, doi:10.1029/2006PA001400.

Scholl, D.W., Stevenson, A.J., Noble, M.A., and Rea, D.K., 2003, The Meiji Drift Body and late Paleogene–Neogene paleoceanography of the North Pacific–Bering Sea region, *in* Prothero, D.R., et al., eds., From greenhouse to icehouse: The marine Eocene-Oligocene transition: New York, Columbia University Press, p. 119–153.

Sclater, J.G., Anderson, R.N., and Bell, M.L., 1971, Elevation of ridges and evolution of the central eastern Pacific: Journal of Geophysical Research, v. 76, p. 7888–7915, doi:10.1029/JB076i032p07888.

Sempson, G.G., 1947, Holoartic mammalian faunas and continental relationship during the Cenozoic: Geological Society of America Bulletin, v. 58, p. 613–687, doi:10.1130/0016-7606(1947)58[613:HMFACR]2.0.CO;2.

Sexton, P.F., Wilson, P.A., and Norris, R.D., 2006, Testing the Cenozoic multisite composite $\delta^{18}O$ and $\delta^{13}C$ curves: New monospecific Eocene records from a single locality, Demerara Rise (Ocean Drilling Program Leg 207): Paleoceanography, v. 21, PA2019, doi:10.1029/2005PA001253.

Shipboard Scientific Party, 1993, Site 884, *in* Rea, D.K., et al., Proceedings of the Ocean Drilling Program, Initial reports, Volume 145: College Station, Texas, Ocean Drilling Program, p. 209–302, doi:10.2973/odp.proc.ir.145.108.1993.

Shipboard Scientific Party, 1998, Site 1053, *in* Norris, R.D., et al., Proceedings of the Ocean Drilling Program, Initial reports, Volume 171B: College Station, Texas, Ocean Drilling Program, p. 321–348, doi:10.2973/odp.proc.ir.171b.107.1998.

Shipboard Scientific Party, 2002, Site 1209, *in* Bralower, J.T., et al., Proceedings of the Ocean Drilling Program, Initial reports, Volume 198: College Station, Texas, Ocean Drilling Program, p. 1–102, doi:10.2973/odp.proc.ir.198.105.2002.

Sijp, W.P., and England, M.H., 2004, Effect of the Drake Passage throughflow on global climate: Journal of Physical Oceanography, v. 34, p. 1254–1266, doi:10.1175/1520-0485(2004)034<1254:EOTDPT>2.0.CO;2.

Sijp, W.P., and England, M.H., 2005, Role of the Drake Passage in controlling the stability of the ocean's thermohaline circulation: Journal of Climate, v. 18, p. 1957–1966, doi:10.1175/JCLI3376.1.

Stabeno, P.J., Schumacher, J.D., and Ohtani, K., 1999, The physical oceanography of the Bering Sea, *in* Loughlin, T.R., and Ohtani, K., eds., Dynamics of the Bering Sea: Fairbanks, University of Alaska Sea Grant, AK-SG-99-03, p. 1–28.

Stickley, C.E., Brinkhuis, H., Schellenberg, S.A., Sluijs, A., Röhl, U., Fuller, M., Grauert, M., Huber, M., Warnaar, J., and Williams, G.L., 2004, Timing and nature of the deepening of the Tasmanian Gateway: Paleoceanography, v. 19, PA4027, doi:10.1029/2004PA001022.

Thomas, D.J., 2004, Evidence for deepwater production in the North Pacific Ocean during the early Cenozoic warm interval: Nature, v. 430, no. 6995, p. 65–68, doi:10.1038/nature02639.

Thomas, D.J., Lyle, M., Moore, T.C., and Rea, D.K., 2008, Paleogene deepwater mass composition of the tropical Pacific and implications for thermohaline circulation in a greenhouse world: Geochemistry, Geophysics, Geosystems, v. 9, Q02002, doi:10.1029/2007GC001748.

Thomas, E., 2007, Cenozoic mass extinctions in the deep sea: What disturbs the largest habitat on Earth?, *in* Monechi, S., et al., eds., Large ecosystem perturbations: Causes and consequences: Geological Society of America Special Paper 424, p. 1–24, doi:10.1130/2007.2424(01).

Toggweiler, J.R., and Bjornsson, H., 2000, Drake Passage and palaeoclimate: Journal of Quaternary Science, v. 15, p. 319–328, doi:10.1002/1099-1417(200005)15:4<319::AID-JQS545>3.0.CO;2-C.

Toggweiler, J.R., and Samuels, B., 1995, Effect of Drake Passage on the global thermohaline circulation: Deep-Sea Research, v. 42, p. 477–500, doi:10.1016/0967-0637(95)00012-U.

Toggweiler, J.R., and Samuels, B., 1998, On the ocean's large-scale circulation near the limit of no vertical mixing: Journal of Physical Oceanography, v. 28, p. 1832–1852, doi:10.1175/1520-0485(1998)028<1832:OTOSLS>2.0.CO;2.

Tripati, A., Backman, J., Elderfield, H., and Ferretti, P., 2005, Eocene bipolar glaciation associated with global carbon cycle changes: Nature, v. 436, no. 7049, p. 341–346, doi:10.1038/nature03874.

van de Flierdt, T., Frank, M., Halliday, A.N., Hein, J.R., Hattendorf, B., Günther, D., and Kubic, P.W., 2004, Deep and bottom water export from the Southern Ocean to the Pacific over the past 38 million years: Paleoceanography, v. 19, PA1020, doi:10.1029/2003PA000923.

van Morkhoven, F.P.C.M., Berggren, W.A., and Edwards, A.S., 1986, Cenozoic cosmopolitan deep-water benthic foraminifera: Pau, France, Elf-Aquitaine, 421 p.

Via, R.K., and Thomas, D.J., 2006, Evolution of Atlantic thermohaline circulation: Early Oligocene onset of deep-water production in the North Atlantic: Geology, v. 34, p. 441–444, doi:10.1130/G22545.1.

Wade, B.S., and Pearson, P.N., 2008, Planktonic foraminiferal turnover, diversity fluctuations and geochemical signals across the Eocene/Oligocene boundary in Tanzania: Marine Micropaleontology, v. 68, p. 244–255, doi:10.1016/j.marmicro.2008.04.002.

Wade, B.S., Houben, A.J.P., Quaijtaal, W., Schouten, S., Rosenthal, Y., Miller, K.G., Katz, M.E., Wright, J.D., and Brinkhuis, H., 2012, Multiproxy record of abrupt sea-surface cooling, across the Eocene-Oligocene transition in the Gulf of Mexico: Geology, v. 40, p. 159–162, doi:10.1130/G32577.1.

Warner, M.J., and Roden, G.I., 1995, Chlorofluorocarbon evidence for recent ventilation in the deep Bering Sea: Nature, v. 373, no. 6513, p. 409–412, doi:10.1038/373409a0.

Warren, B.A., 1983, Why no deep water formed in the North Pacific: Journal of Marine Research, v. 41, p. 327–347, doi:10.1357/002224083788520207.

Woodruff, F., and Savin, S.M., 1989, Miocene deepwater oceanography: Paleoceanography, v. 4, p. 87–140, doi:10.1029/PA004i001p00087.

Wright, J.D., Miller, K.G., and Fairbanks, R.G., 1992, Early and middle Miocene stable isotopes: Implications for deepwater circulation and climate: Paleoceanography, v. 7, p. 357–389, doi:10.1029/92PA00760.

Yu, J., and Elderfield, H., 2008, Mg/Ca in the benthic foraminifera *Cibicidoides wuellerstorfi* and *Cibicidoides mundulus*: Temperature versus carbonate ion saturation: Earth and Planetary Science Letters, v. 276, p. 129–139, doi:10.1016/j.epsl.2008.09.015.

Zachos, J., Breza, J.R., and Wise, S.W., 1992, Early Oligocene ice-sheet expansion on Antarctica: Stable isotope and sedimentological evidence from Kerguelen Plateau, southern Indian Ocean: Geology, v. 20, p. 569–573, doi:10.1130/0091–7613(1992) 020<0569:EOISEO> 2.3.CO;2.

Zachos, J., Stott, L.D., and Lohmann, K.C., 1994, Evolution of the early Cenozoic marine temperatures: Paleoceanography, v. 9, p. 353–387, doi:10.1029/93PA03266.

Zachos, J.C., Quinn, T.M., and Salamy, K.A., 1996, High-resolution ($10^4$ years) deep-sea foraminiferal stable isotope records of the Eocene-Oligocene climate transition: Paleoceanography, v. 11, p. 251–266, doi:10.1029/96PA00571.

Zachos, J., Pagani, M., Sloan, L., Thomas, E., and Billups, K., 2001, Trends, rhythms and aberration in global climate 65 Ma to present: Science, v. 292, no. 5517, p. 686–693, doi:10.1126/science.1059412.